12-9-2022

Quantifying Carbon Dioxide and Methane Fluxes from Sargassum Strandings on Florida Beaches

James O. Westphalen

Thesis of
James O. Westphalen

Submitted in Partial Fulfillment of the Requirements for the Degree of

Master of Science
Marine Science

Nova Southeastern University
Halmos College of Arts and Sciences

December 2022

Approved:
Thesis Committee

Committee Chair: Tyler Cyronak

Committee Member: Joana Figueiredo

Committee Member: Rosana Boyle

HALMOS COLLEGE OF ARTS AND SCIENCE

Quantifying Carbon Dioxide and Methane Fluxes from *Sargassum* Strandings on Florida Beaches

James Westphalen

Submitted to the Faculty of

Halmos College of Arts and Sciences

in partial fulfillment of the requirements for

The degree of Master of Science with a specialty in:

Marine Biology

Nova Southeastern University

December, 2022

Abstract:

Floating *Sargassum* is thought to be a sink of blue carbon in that it removes carbon dioxide (CO_2) from the atmosphere and sequesters organic carbon by sinking into the deep ocean or being buried in sediments. However, *Sargassum* that washes into intertidal ecosystems will eventually decompose, releasing greenhouse gases to the surrounding air, groundwater, and surface coastal seawater. In recent years, *Sargassum* strandings have increased in the Atlantic Ocean, making our understanding of the fate of beached Sargassum critical for determining how much carbon is sequestered by the seaweed. This study investigated greenhouse gas fluxes of decaying *Sargassum* wrack in mesocosm experiments to understand how beached *Sargassum* could affect the coastal carbon cycle. GHG fluxes were investigated in two mesocosm experiments, simulating (1) tidal seawater inundation of *Sargassum* wrack and (2) wrack decomposing in oxygen restricted and aerated conditions. Measurements of greenhouse gas fluxes from naturally decomposing *Sargassum* were also undertaken. Overall, strong CO_2 fluxes were recorded with weak or inconsistent CH_4 fluxes. Simulated tidal conditions and simulated hypoxic conditions did not lead to differences in GHG fluxes, though dry conditions did have greater CO_2 fluxes than seawater immersion conditions. Over the course of the experiment, alkalinity in seawater mesocosms increased, likely due to anaerobic chemical pathways. *In-situ* incubations of stranded *Sargassum* returned strong CO_2 and CH_4 fluxes, although it is unclear whether these were due to the wrack itself or underlying sediment biogeochemical processes.

Keywords: Biogeochemistry · Blue Carbon · Carbon Sequestration · Methanogenesis · Carbonate Chemistry · Macroalgae · Decomposition

Table of Contents

List of Tables

List of Figures.

Introduction

Anthropogenic climate change is responsible for many disruptions in the Earth system, including global warming, changes in weather patterns, ocean acidification, and sea level rise (Mikaylov et al. 2020). Human perturbations to the global carbon cycle are the main cause of modern climate change, which is largely driven by the buildup of fossil fuel derived greenhouse gases in the atmosphere (Mikaylov et al. 2020).). Greenhouse gases (GHG) induce a warming effect by trapping longwave radiation and emitting it back to the Earth's surface and atmosphere. The major driver of modern climate change is carbon dioxide (CO_2), which has a long residence time in the atmosphere (>500 years) (Archer 2005). Other important anthropogenic GHGs include methane (CH_4) and nitrous oxide (N_2O). Both CH_4 and nitrous oxide have higher warming potentials than CO_2, but have shorter residence times due to destructive chemical reactions that occur in the atmosphere (Boucher et al. 2009, Fuglestvedt et al. 1996). Over time scales less than 100 years, CH_4 has a global warming potential 27 times that of CO_2 (Boucher et al. 2009). The main anthropogenic sources of CH_4 include livestock, agriculture, and landfills, while CH_4 is naturally produced in marine ecosystems such as mangrove swamps and seagrass meadows (Garcias-Bonet & Duarte 2017, Rosentreter et al. 2017). In total, the sum of all anthropogenic GHG emissions have led to a global warming of 1.07° C over the past century, and the trend is expected to continue depending on future emission scenarios (IPCC 2021).

CO_2 is naturally cycled through natural processes in the carbon cycle, and certain ecosystems are net sinks for this gas. In general, ecosystems with net-negative CO_2 emissions are called green carbon ecosystems, of which 45% of the carbon stored exists in terrestrial ecosystems, and 55% in aquatic ecosystems (Nelleman et al. 2009). Net-negative CO_2 marine ecosystems are often referred to as blue carbon ecosystems (Nelleman et al. 2009). It is estimated that 111 Tg of carbon are buried per year by marine vegetation (Duarte et al. 2005). Blue carbon ecosystems include but are not limited to salt marshes, mangrove swamps, seagrass meadows and macroalgae forests (Nelleman et al. 2009, Siikamäki et al. 2013). These ecosystems are often characterized by high internal carbon burial rates and accumulation of carbon in soils and sediments (Filbee-Dexter & Wernberg 2020). Angiosperm-dominated blue carbon ecosystems even bury carbon at a rate 40 times more than tropical rainforests (Duarte et al. 2005). In most of

these ecosystems, the carbon is buried in coastal sediments, but macroalgae ecosystems tend to store carbon by exporting it to the deep ocean.

Macroalgal ecosystems differ from other recognized blue carbon sinks in that they do not produce carbon-rich sediments. Angiosperm-dominated ecosystems such as seagrass meadows or mangrove swamps can store carbon below ground in both living roots and rhizomes as well as non-living detrital material in the sediment (Rosentreter et al. 2018). Macroalgae sequestration is difficult to track, as much of the carbon stock within a macroalgal ecosystem is present as living tissue and is often not buried on site once the organism dies (Krause-Jensen & Duarte 2016). Since many habitat-forming macroalgae are neutrally buoyant, once detached from substrate the thalli are readily exported to other marine ecosystems (Krause-Jensen & Duarte 2016, Kokubu et al. 2019). In general, organic carbon captured as macroalgal biomass can either be buried in sediments on the continental shelf or exported to the deep ocean (Krumhansl & Shiebling 2012). Through this burial process, macroalgal ecosystems sequester around 173 Tg yr^{-1} of carbon per year (Krause-Jensen & Duarte 2016). As macroalgae and their degradation products sink below the thermocline into the mesopelagic ocean, carbon fixed as particulate organic carbon or dissolved organic carbon (POC and DOC, respectively) becomes isolated from the atmosphere and contributes to long term sequestration (Filbee &Wernberg 2020). This long-term deep ocean sequestration of carbon accounts for up to 88% of carbon sequestered by macroalgae (Krause-Jensen & Duarte 2016, Kokubu et al 2019). Species of macroalgae with the potential for long range transport, such as *Sargassum spp*., are the most effective at capturing and transferring carbon to the deep ocean (Kokubu et al. 2019). This includes benthic forms with gas-filled vesicles that cause the macroalga to float after detachment, as well as pelagic forms that float throughout their lifespan. This is because these species tend to grow in coastal habitats with high nutrient availability, and the ability for long range transport allows these macroalgae to be carried to offshore zones, where they can sink below the mixed layer and sequester their carbon on long term scales. Any carbon that is sequestered in the deep ocean can potentially be sequestered for up to 1,000 years (Nelleman et al. 2009).

Sargassum, a genus of brown macroalgae, grows either in coastal benthic forests or in pelagic rafts on the open ocean. Benthic *Sargassum* forests dominate tropical canopy forming macroalgal habitats, and pelagic species create biodiverse floating habitats in the northern

Atlantic gyre (the Sargasso Sea) and the Caribbean Sea (Krause-Jensen & Duarte 2016). There are many benthic *Sargassum* species (e.g. *S. fusiforme, S. horneri, S. vulgare*) but there are two common pelagic species, *Sargassum natans* and *Sargassum fluitans*. Pelagic *Sargassum* species have no holdfast and reproduce by vegetative fragmentation in the open ocean. They provide nursery space and habitat for pelagic animals, supporting complex food webs that are essential to biodiversity in the oligotrophic open ocean (Martin et al. 2021). *Sargassum* itself is not often consumed by inhabitants of raft communities (Turner & Rooker 2006), as the macroalga produces compounds that deter herbivory (Li et al. 2017). Despite not serving as a direct food source, *Sargassum* provides energy to the surrounding habitat by releasing dissolved organic carbon (DOC) that can be absorbed by the bacteria and plankton that serve as the base of the food web (Powers et al. 2019). Sargassum forests and raft communities contain 13.1 Pg of carbon globally, which is similar in biomass to the carbon held by salt marshes, and almost twice the biomass held by mangroves and seagrasses (Gouvea et al. 2020). Due to the comparatively large amount of carbon stored in living *Sargassum*, this global sink of carbon has been referred to as golden carbon (Gouvea et al. 2020, Kwan et al. 2022).

The main pathway for sequestering carbon in neutrally buoyant macroalgae is through sinking below the mixed layer. Macroalgae have been found to concentrate in the flow of a submarine canyon (Josselyn et al. 1983, Krause-Jensen & Duarte 2016), though macroalgae falls in more disperse concentrations over continental shelves (Kokubu et al. 2019). When not concentrated by bottom topography, macroalgae falls can be concentrated by the fronts of main ocean currents (Kokobu et al. 2019). Once macroalgae sink into the deep ocean, the detritus either mineralizes completely or fuels deep sea food webs (Krause-Jensen & Duarte 2016). For instance, pieces of macroalgae such as *Sargassum* have been found in the guts of invertebrates in the abyssal zone as deep as 6,475 m (Lawson 1993, Shoener & Rowe 1970). Sinking of *Sargassum* occurs either as the macroalga itself becomes negatively buoyant due to epibiont weight and the collapse of its vesicles, or as fauna that consume *Sargassum* and *Sargassum*-associated epibionts drop fecal pellets as marine snow (Itoh et al. 2007). As organic carbon is moved from the upper ocean mixed layer to the deep ocean, it is essentially isolated from the atmosphere over long periods of time (Krause-Jensen & Duarte, 2016). *Sargassum* can also sequester carbon through calcite production, which can constitute up to 22% of the macroalga's

ash content, and directly becomes sediment following decomposition (Paraguay-Delgado et al. 2020). However, estimates of the magnitude of carbon sequestered by *Sargassum* vary.

Gouvea et al. (2020) claim that floating *Sargassum* blooms have a major effect on global carbon storage, while Hu et al. (2021) claim that golden carbon sequestration is significant on a local scale but not on a global scale. Hu et al. (2021) claim that although *Sargassum* habitats have 16.7 times the sequestration rate of phytoplankton, the spatial distribution of phytoplankton results in greater primary production over a global scale, and thus greater sequestration rates than the pelagic macroalga. Estimates of macroalgae net primary productivity that is sequestered in the deep sea is currently based on models and may not accurately reflect the actual amount of sequestered carbon (Krause-Jensen et al. 2016). Evidence for deep sea macroalgae sequestration is mostly found through gut sampling of invertebrates (Shoener &Rowe 1970), bottom trawling in relatively shallow depths (Kokubu et al. 2019), and photographs of detritus on the bottom taken by remotely operated or autonomous underwater vehicles (Shoener & Rowe 1970, Baker et al. 2018). It is also difficult to quantify the burial of macroalgae detritus that has been imported into mangrove swamps, seagrass beds and salt marshes, making this another challenge to quantifying the carbon sequestration potential of macroalgal ecosystems (Krause-Jensen et al. 2016).

Apart from direct removal of carbon to burial and to the deep ocean, macroalgae can sequester carbon through anaerobic decomposition, which occurs after macroalgal wrack is washed onto sandy beaches (Erk et al. 2020, Perkins et al. 2022). Processes such as calcium carbonate dissolution, manganese and iron reduction, denitrification and sulfate reduction utilize organic material and release products such as total alkalinity (TA) and dissolved inorganic carbon (DIC) (Borges et al. 2003, Krumin et al. 2013, Erk et al. 2020, Perkins et al. 2022). Decomposition processes also produce POC, labile DOC, and refractory DOC into porewaters under the beach (Erk et al. 2020). As stated earlier, POC and refractory DOC that are exported from macroalgal ecosystems into the deep ocean can become sequestered carbon. In addition to recalcitrant compounds released into porewater, macroalgae stranded above the normal high tide line can serve as a temporary sink for decomposition products, as low moisture and few inundation events leads to lower rates of recycling of these decomposition products (Lastra et al. 2018). Living macroalgae also export carbon as DOC and POC which can be sequestered

through burial in other ecosystems or through sinking into the deep ocean. About 43% of the net primary productivity of macroalgae is exported as DOC and POC (Duarte & Cebrian 1996, Krause- Jensen et al. 2016). Living macroalgae produce 5-20% of their NPP as refractory DOC, or DOC that is not readily broken down in the water column, as opposed to labile DOC (Watanabe et al. 2020). Macroalgae produce DOC that is much more recalcitrant than that of phytoplankton (Wada et al. 2008), making macroalgal ecosystems important contributors to DOC dynamics within the ocean. Although all DOC in the epipelagic ocean is eventually mineralized (Lechtenfeld et al. 2013), if DOC down wells into the mesopelagic ocean it can sequester carbon for longer time periods.

Although blue carbon ecosystems have high carbon burial rates, they can also have high CO_2 and CH_4 emission rates, which can lower their CO_2 sequestration potential (Rosentreter et al. 2018). In addition to the release of GHGs through natural processes, coastal blue carbon ecosystems that are disturbed or destroyed by anthropogenic activities lose sequestering potential and begin to release GHG from old carbon stores (Duarte et al. 2005, Pendleton et al. 2012). Buried organic carbon material decomposes faster when it is exposed to oxygen, leading to quicker release of GHGs (Pendleton et al. 2012). It is estimated that 0.45 Pg of CO_2 are released from disturbed blue carbon ecosystems each year (Pendleton et al. 2012) and CH_4 release from degraded mangrove swamps may play a particularly important role in climate change (Rosentreter et al. 2018). Therefore, it is critical to assess the fluxes of GHGs from blue carbon ecosystems to determine how they may relate to global CO_2 emissions.

As *Sargassum*'s overall contribution to blue carbon is poorly understood, changes in this ecosystem's sequestration and emission of carbon may give a better picture of blue carbon dynamics on a global scale. A challenge to understanding the dynamics of golden carbon sequestration is the recent change in the growth and distribution of floating *Sargassum.* Blooms have occurred in greater frequency and biomasses in the Equatorial Atlantic since 2011 (Wang et al. 2019). These blooms have occurred in the summer months, most notably in July, and collectively form the Great Atlantic *Sargassum* Belt (GASB). The GASB increased by an average of 139.6 million tons in biomass each year from 2011 to 2018, although it did not increase in biomass every consecutive year (Wang et al. 2019). It is not clear what has caused this increase, but hypotheses include changes in upwelling in the eastern Atlantic, higher

nitrogen concentrations in the Atlantic from land-based runoff in the Amazon catchment (Lapointe et al. 2021), or higher iron concentrations originating from ore mining runoff (Gouvea et al. 2020). Regardless of the causes of increased *Sargassum* over recent decades, this phenomenon could lead to changes in the amount of golden carbon that is sequestered on a yearly basis.

Although the majority of pelagic *Sargassum* remain in the open ocean, large amounts of *Sargassum* do not sink to the deep ocean and often wash up onto beaches, becoming stranded. This is becoming an increasing problem in the Caribbean and Gulf of Mexico region as the pelagic biomass of *Sargassum* increases stranding events (van Tussenbroek et al. 2017, Wang et al. 2019, Hernández et al. 2021). Since stranded *Sargassum* does not sink into the mesopelagic ocean, its decomposition can have a direct impact on the atmosphere and nearby coastal waters. The decomposition of stranded *Sargassum* can have many ecological consequences including dissolved oxygen consumption, increased sulfide reduction, CO_2 and CH_4 production, and direct negative impacts on organisms utilizing beach habitat as well as on organisms living near affected coasts (Maurer et al. 2015, Resiere et al. 2018, Erk et al. 2020). Decomposing macroalgae produce GHG such as CO_2 through aerobic decomposition and CH_4 through anaerobic respiration (Lastra et al. 2018, Erk et al. 2020, Perkins et al. 2022). From the perspective of carbon burial, the CO_2 that is produced through aerobic decomposition replaces the CO_2 that was removed from the atmosphere by photosynthesis, resulting in a net zero impact on the carbon cycle. CH_4 has a greater greenhouse warming impact than CO_2 on a 100-year timescale, so any CH_4 that is released through decomposition pathways has the potential to offset carbon burial over the short term. For instance, CH_4 has been shown to offset the global benefits of carbon sequestration by 18% to 22% in mangrove forests (Rosentreter et al. 2018) and by 4.8% in seagrass beds (Garcias-Bonet & Duarte 2017). Though a study that evaluates the natural GHG emissions of *Sargassum* has not yet been done, macroalgae wrack are known to undergo methanogenesis under anaerobic conditions (Erk et al. 2020, Perkins et al. 2022). Methanogenesis is only one of many anaerobic processes that can occur when organic matter decomposes on a beach. Fermentation and hydrolysis are important in breaking down the complex molecules that macroalgae produce (Erk et al. 2020). Sulfate reduction on beaches is the main driver of kelp decomposition, but this does not occur without mixing of kelp and the beach sand (Erk et al. 2020). The degradation of macroalgae on beaches also exports carbon in

the form of DOC, DIC and alkalinity (Perkins et al. 2022). If these products remain dissolved in ocean water, they could become a carbon sequestering process.

In addition to GHGs released from decomposition, *Sargassum* strandings have direct negative effects on beaches that they wash onto. Sulfate reduction leads to the release of hydrogen sulfide, a foul-smelling and toxic gas (Gray et al. 2021). Humans that breathe this gas can contract hypoxic pulmonary, neurological, and cardiovascular lesions (Resiere et al. 2018). Since the South Florida economy relies heavily on tourism, *Sargassum* strandings cause economic losses (Gray et al. 2021) and require extensive efforts to be removed from beaches (Resiere et al. 2018). In addition to negative health effects on human populations, excessive decomposing *Sargassum* has negative health effects on beach and near-shore communities. Decaying *Sargassum* releases tannins and particulate organic matter (van Tussenbroek et al. 2017), which increase water turbidity and limit the light that photosynthetic organisms such as seagrasses and scleratinian corals require. Oxygen concentrations and pH decrease, as aerobic decomposition consumes oxygen and releases CO_2 to the water (van Tussenbroek et al. 2017). In the height of a stranding event on Mexican Caribbean beaches in 2015, decaying *Sargassum* added approximately 30 times the amount of nitrogen and approximately 3-10 times the amount of phosphorous that is normally exported to near-shore waters by terrestrial runoff (van Tussenbroek et al. 2017). In 2018, a *Sargassum* bloom caused a mass mortality of marine fauna in Mexico by increasing dissolved hydrogen sulfide and ammonium, and causing hypoxic conditions (Rodríguez-Martínez et al. 2019). *Sargassum* inundations indirectly lead to beach erosion, as the decomposition of *Sargassum* may kill nearshore seagrass communities that would normally reduce erosion, and removal efforts by humans can damage beach structure (van Tussenbroek et al. 2017). Piling of *Sargassum* also excludes use of beaches by sea turtles, limiting their nesting habitat (Maurer et al. 2015).

Recent increases in *Sargassum* biomass in the Atlantic has led to increased stranding events on beaches and increases in subsequent decomposition. This increase in stranded biomass necessitates a better understanding of how decomposing *Sargassum* impacts coastal biogeochemical cycles. Methanogenesis is a process inherent to anaerobic zones in macroalgal wrack, and is likely to occur in stranded mats of *Sargassum*. As both aerobic and anaerobic decomposition of *Sargassum* increase on a global scale, the GHG fluxes of this process may also

give a better picture of this process's role in global carbon and GHG dynamics. In this study the atmospheric CO_2 and CH_4 fluxes and carbonate chemistry from beached *Sargassum* wrack were examined through different methods. CO_2 and CH_4 fluxes were measured using chamber incubations on wrack stranded on a South Florida beach, as well as through a time series of *Sargassum* decomposition in experimental mesocosms. The same mesocosms were used to track changing carbonate chemistry throughout the decomposition process. Overall, this study seeks to understand carbon fluxes from stranded *Sargassum*, and how the expected increasing frequency of stranding events may change dynamics of blue carbon in coming years.

Methods

Overall experimental design and sampling

The focus of this study was on two separate ex-situ experiments, each including 12 mesocosms that were an attempt to determine GHG emission rates from decaying *Sargassum* under different scenarios. Experiment 1 was carried out before Experiment 2, with the same 12 mesocosms used in Experiment 1 being used again in Experiment 2. Mesocosm design is shown in Figure 2. Bulk mats of floating *Sargassum* biomass were collected off the coast of Ft. Lauderdale, Florida on two different days, June 15th 2022 for Experiment 1 and July 21st 2022 for Experiment 2. Fresh *Sargassum* was retrieved approximately 1.5 km offshore via small boat and brought back to the laboratory for processing. Approximately 1 kg of *Sargassum* material, including epibionts, were deposited into each mesocosm. Some mesocosms also included seawater, which was sourced an aquarium shop that collects seawater from offshore of Ft. Lauderdale. After *Sargassum* was added, mesocosms were left for ca. 21 hours before the first incubation was started. Mesocosms were closed in a way that reduced evaporation of seawater and blocked light. Aeration of certain mesocosms was done by pushing air into the airspace using a Tetra 3.3 L min^{-1} aquarium pump. When incubations began, mesocosms were opened to bring the internal GHG concentrations to an ambient atmospheric level. After equalization to atmospheric gas levels, the lid to the mesocosm was sealed and connected by valves to a LiCOR 7810 trace gas analyzer (CO_2 and CH_4 emissions), which was used to determine the change of GHG concentrations in the bucket over time. Each incubation lasted from 5-15 minutes, with the intention of recording a linear increase or decrease of the target gases which could be converted to fluxes. Fluxes were later calculated using Equation 1.

Experiment 1 Design

To determine whether tidal inundations of beached *Sargassum* affect GHG flux, Experiment 1 investigated the effects of seawater immersion, dry conditions and simulated tidal inundation on *Sargassum* wrack in mesocosms. In this experiment, there were three experimental treatments (Figures 1 & 2), each with four replicates. The three treatments during this experiment were: dry *Sargassum* (no seawater added to buckets), *Sargassum* immersed in seawater with no pumping, and a custom-built pump system that sprayed seawater from the bottom of the mesocosm onto *Sargassum* that was elevated from the reservoir by a plastic framework, meant to

simulate the inundation and desiccation cycle that wrack in the intertidal zone on beaches are subjected to. The pump system sprayed seawater from a reservoir below the *Sargassum* for 12 hours before turning off for another 12 hours, repeating over the extent of the experimental period. All three treatments included pumping of ambient atmospheric air into the mesocosms. The experiment lasted 15 days (June 16th to June 30th 2022), and mesocosms were sampled every 2-4 days for CO_2 and CH_4 concentrations from the mesocosm, following the methods in overall design and sampling. The first experiment resulted in six days of GHG emissions collected from the twelve total mesocosms. Chamber heights from the top of the *Sargassum* to the top of the mesocosm were recorded to later use as chamber heights in the flux equation (equation 1).

Experiment 2 Design

To determine how anaerobic conditions affect GHG flux from *Sargassum* wrack, Experiment 2 investigated the difference between aerating the wrack and sealing the wrack in a hypoxic environment. In this experiment there were four experimental conditions with three replicates each. The experimental conditions included dry and seawater filled mesocosms with or without aeration of the mesocosms. Aerated buckets had ambient atmospheric air pumped into them throughout the decomposition experiment, while closed buckets were sealed until data were collected. Over the course of 21 days (July 22nd to August 11th 2022), mesocosms were sampled every 2-4 days for CO_2 and CH_4 concentrations (Figure 1), resulting in seven days of data collection. Chamber heights were recorded from the top of the *Sargassum* to the top of the bucket, to later be used in the flux equation (equation 1). Water temperature and oxygen content was also recorded in the seawater buckets using a Hach HQ40 digital multimeter. Mesocosms with seawater were sampled for later chemical analysis of total alkalinity and pH (15mL). These water samples were treated with mercuric chloride and stored in borosilicate glass bottles according to best practices (Dickson et al. 2007). An 888 Titrando Metrohm titrator with an 806 Dosimat and Metrohm pH electrode were used to measure pH and calculate alkalinity using potentiometric acid titration, as per Cyronak et al. (2013).

Figure 1. Pictures of (A) mesocosms, (B) *Sargassum* at start of experimental period, and (C) *Sargassum* at end of experimental period in experiment 2.

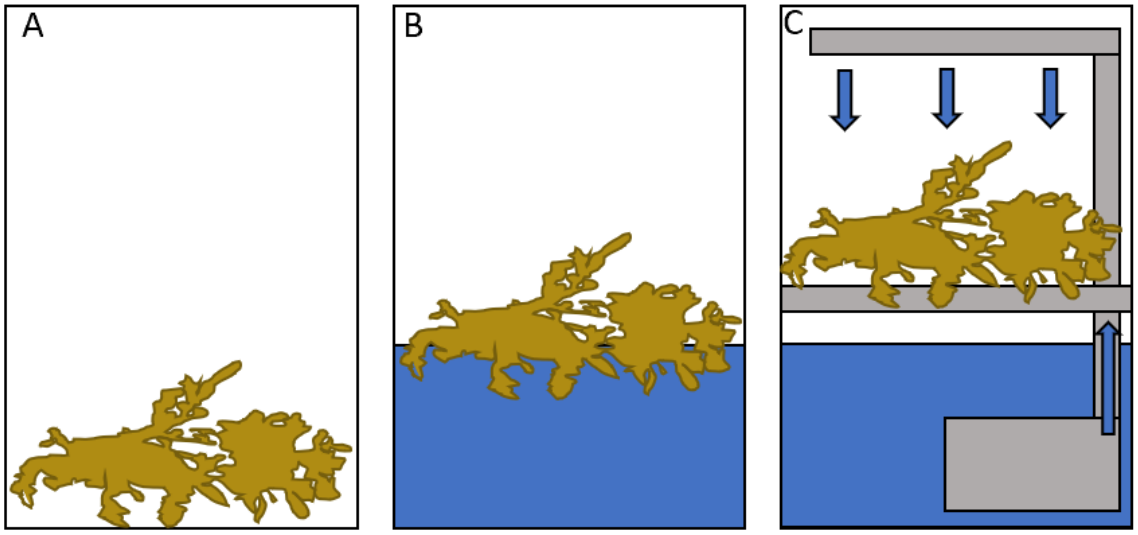

Figure 2. Mesocosm design in the different experiments. (A) Dry experimental conditions, (B) seawater experimental conditions, and (C) simulated tidal conditions. The brown shape represents the *Sargassum*, the blue box represents seawater and white space represents empty space in the mesocosm. All three were used in Experiment 1, while only the dry and seawater designs were used in Experiment 2. In Experiment 2, dry and seawater conditions were crossed with aerated and closed conditions.

Beach incubation Design

Gas emission data was acquired from *Sargassum* wrack that was washed onto the beach of the Dr. Von D. Mizell-Eula Johnson State Park, located in Broward County of Florida (Figure 3). *Sargassum* rafts often wash onto this beach in large quantities (Figure 4) following blooms in summer months, making it an ideal location for this study. The incubation chamber used was a custom built 4-inch diameter, 2-foot-long PVC pipe, which was capped at the top and had valves for connections to the LiCOR 7810 trace gas analyzer (Figure 5). This incubation chamber was placed on top of selected sites, and where necessary it was pushed through deep wrack to rest on the sand itself. As with the mesocosm incubations, air within the incubation chamber was aired out and returned to ambient atmospheric gas concentrations before beginning the next incubation. An in-line Drierite chamber was used to dry the gas before it entered the LiCOR 7810. The first beach sampling was done on September 9th, 2022. Four different sites were sampled for GHG flux: dry sand as a control, dry wrack at a depth of 304mm, shallow and wet wrack at a depth of 51mm (shown in figure 5), and deep and wet wrack at a depth of 559mm. The second beach sampling was done on October 19th, 2022. Three different sites were sampled for GHG flux: dry sand as a control, wet shallow wrack between 15 and 80 mm, and wet deep wrack between 180 and 290 mm. Three replicates of each type of site were sampled.

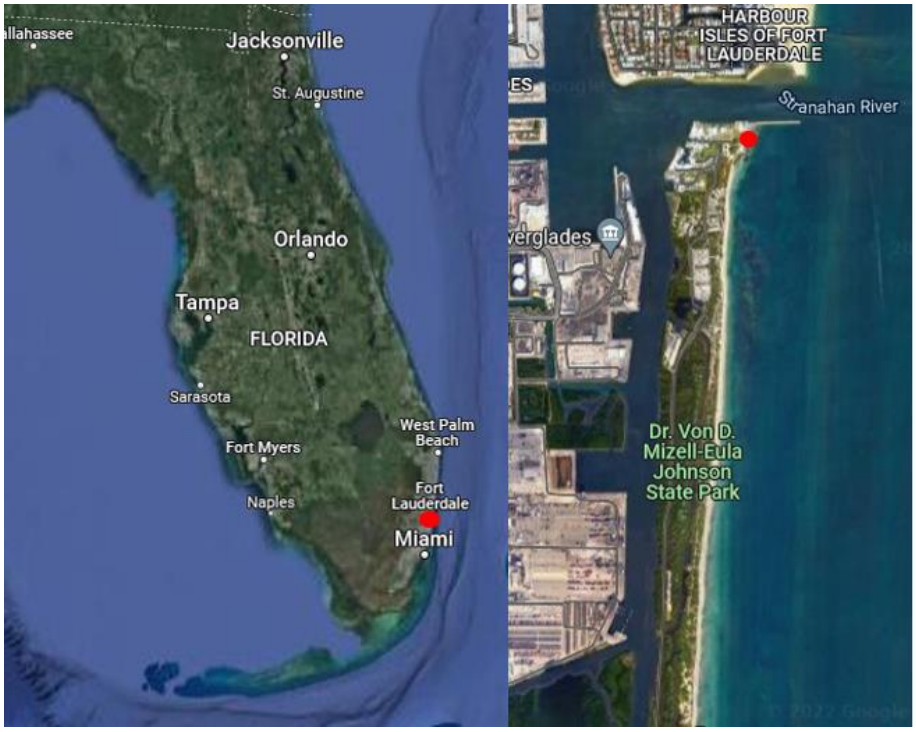

Figure 3. Map of location of Dr. Von D. Mizell-Eula State Park, the sampling site within the park for *Sargassum* wrack, shown here as a red dot. Coordinates are 26.09° N, 80.11° W.

Figure 4. *Sargassum* wrack stranded on beach of the Dr. Von D. Mizell-Eula Johnson State Park in the Summer of 2022.

.

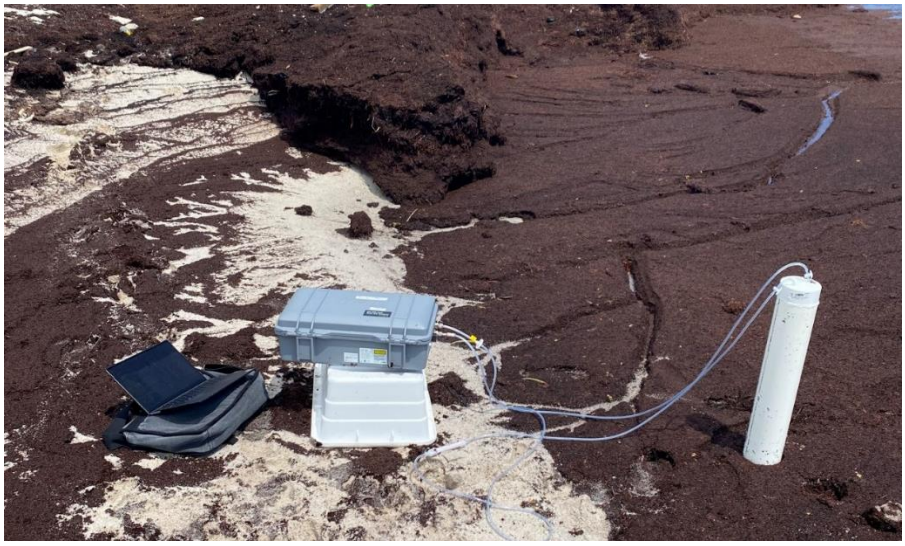

Figure 5. Gas emission data acquisition of shallow *Sargassum* wrack on beach, using LiCOR trace gas analyzer.

Data Analysis

To find rates of GHG flux in each sample, once the CO_2 and CH_4 data were collected from the beach and mesocosm experiments, linear regressions were done in R. GHG fluxes were determined using equation 1 (Sippo et al. 2020);

$$Flux = \left(s\left[\frac{V}{RT_{air}A}\right]\right) \quad \text{(Equation 1)}$$

Where: *S* is the slope of the linear regression between time and gas concentration (Fig. 6),

V is the volume of the headspace above the wrack (L),

R is the universal gas constant (8.205×10^{-5} m^3 atm $K^{-1}mol^{-1}$),

T_{air} is the air temperature in Kelvin, and

A is the surface area of the wrack in the mesocosm (m^2).

The flux values are presented in µmol m^{-2} s^{-1} for CO_2 and nmol m^{-2} s^{-1} for CH_4.

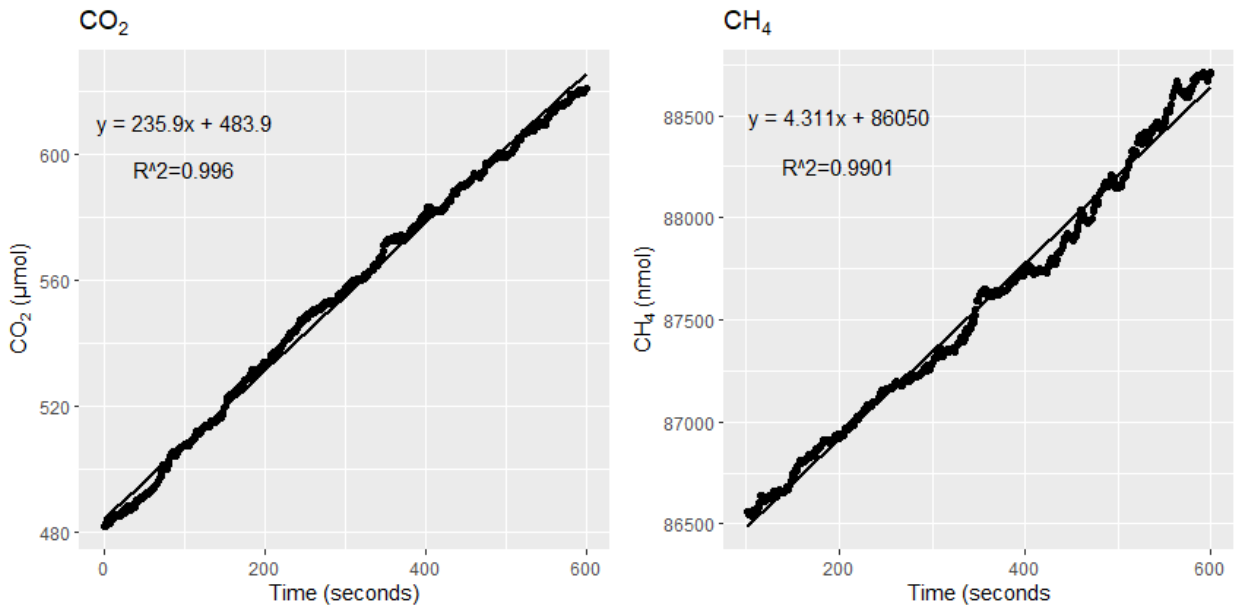

Figure 6. Example CO_2 and CH_4 emission data from a beach incubation, concentrations are in µmol for CO_2 and nmol for CH_4. The slope of the line was determined in R and used in the flux calculations.

Only incubations with a linear relationship between time and gas concentration could be converted to flux. Any linear regression that did not have a linear regression with an R^2 greater than or equal to 0.9 were removed from analysis, as per Sippo et al. (2020). Eight CO_2 incubations were removed from Experiment 1 data. Fifty-nine CH_4 incubations were also removed from Experiment 1 data, resulting in the CH_4 data from this experiment not being converted to fluxes. Three CO_2 incubations and 12 CH_4 incubations were removed from Experiment 2 data.

To determine whether treatments caused significantly different GHG fluxes, non-parametric tests were used, due to both the flux data and transformed flux data being non-normal. For this reason, Kruskal-Wallis tests were used for both experiment 1 and experiment 2 for GHG fluxes. GHG fluxes were not individually analyzed by experimental condition over time.

To determine whether aerated and closed treatments caused significantly different dissolved oxygen concentrations, TA and pH in experiment 2, non-parametric tests were also used as data and transformed data had non-normal distributions. Wilcoxon rank sum tests were used for this purpose. To determine whether these variables changed over time within each

condition group, one-way repeated measures ANOVAs were used to account for repeated measured within each condition. Aligned rank transformation ANOVAs were used as a post hoc test, from using r packages ARTool and rcompanion.

To analyze what biogeochemical processes (Table 1) were occurring during decomposition, TA was compared to DIC for both seawater experimental conditions. DIC was calculated using CO_2SYS adapted for Excel (Pierrot et al. 2006) with dissociation constants of Mehrbach et al. (1973), refit by Dickson & Millero (1987) and the NBS scale. The correlation found for TA:DIC was compared to known stoichiometric values for biogeochemical processes: sulfate reduction, calcium carbonate dissolution, manganese and iron reduction and denitrification (Table 1), as per Borges et al. (2003). These reactions and **Δ**TA and **Δ**DIC values were adapted from Borges et al. (2003), Krumins et al. (2013), Hyun et al. (2017), and Perkins et al. (2022).

Table 1. Biogeochemical processes producing and consuming alkalinity and dissolved inorganic carbon that might be expected in macroalgal wrack decomposition. The corresponding changes in TA and DIC are included alongside the chemical reaction.

Biogeochemical Process	**Reaction**	**ΔTA**	**ΔDIC**
Aerobic Respiration	$(CH_2O)_{106}(NH_3)_{16}(H_3PO_4) \rightarrow 106CO_2+16NO_3 + H_3PO_4$	- 0.2	+ 1
Denitrification	$CH_2O + 0.8NO_3^- + 0.8H^+ \rightarrow CO_2 + 0.4N_2 + 1.4H_2O$	+ 0.8	+ 1
Sulfate reduction	$CH_2O + 0.5SO_4^{2-} + 0.5H^+ \rightarrow CO_2 + 0.5HS^- + H_2O$	+ 1	+ 1
Carbonate dissolution	$CaCO_3 \rightarrow Ca^{2+} + CO_3^{2-}$	+ 2	+ 1
Iron reduction	$CH_2O + 4Fe(OH)_3 + 0.8H^+ \rightarrow CO_2 + 4Fe^{2+} + 11H_2$	+ 8	+ 1
Manganese reduction	$CH_2O + 2MnO_2 + 4H^+ \rightarrow CO_2 + 2Mn^{2+} + 3H_2O$	+ 4.4	+ 1

Results

Experiment 1

For the first mesocosm experiment there were three conditions: dry, wet, and tidal. Over the course of the experiment CO_2 fluxes ranged from -3.0 to 59.5 µmol m^{-2} s^{-1}. In Experiment 1, fluxes were found to be significantly different (Kruskal-Wallis, $p < 0.05$), but a post hoc test did not reveal any significant differences between individual tests. CO_2 flux over time for each treatment is shown in figure 7, and CO_2 flux compared per treatment is shown in figure 8. Fluxes up to as high as 59. 5 µmol m^{-2} s^{-1} occurred in mesocosms with the dry treatment on the first sampling day (fig. 7), after which fluxes fell to ca. 10 µmol m^{-2} s^{-1} and below for the rest of the sampling period.

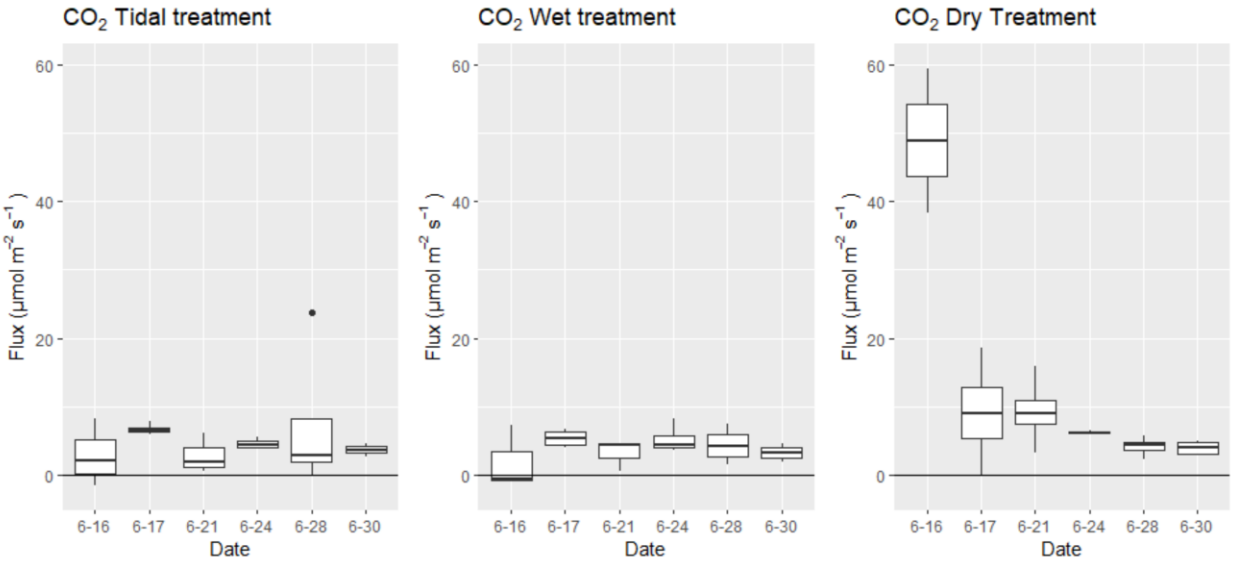

Figure 7. Box plots of CO_2 fluxes from tidal, wet, and dry conditions from experiment 1 taken on each day of sampling.

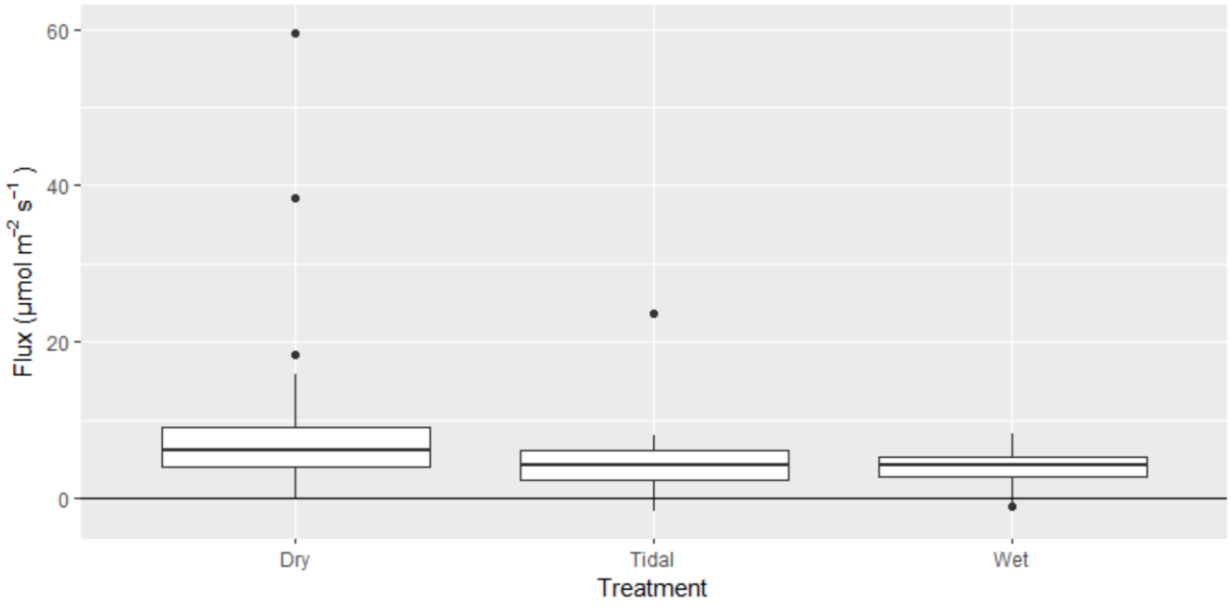

Figure 8. Box plots of CO_2 fluxes separated by the experimental conditions from the first experiment, compiled over every sampling day for each condition.

Experiment 2

In experiment 2, dissolved oxygen concentrations in the wet mesocosms were not found to be significantly different between aerated and closed conditions (Wilcoxon rank-sum, $p = 0.13$). Therefore, it cannot be said that the experimental conditions were truly different between the aerated and non-aerated wet conditions. Dissolved oxygen concentrations in aerated mesocosms were not different per day of sampling (fig. 9, one-way repeated measures ANOVA, $p = 0.18$), although they were different per day of sampling in the closed mesocosms (one-way repeated measures ANOVA, $p < 0.05$). Although dissolved oxygen in the aerated mesocosms had some high outliers on the first day of sampling, this difference was not found to be significantly different. Dissolved oxygen was not measured in the dry conditions, as there was no seawater in these mesocosms.

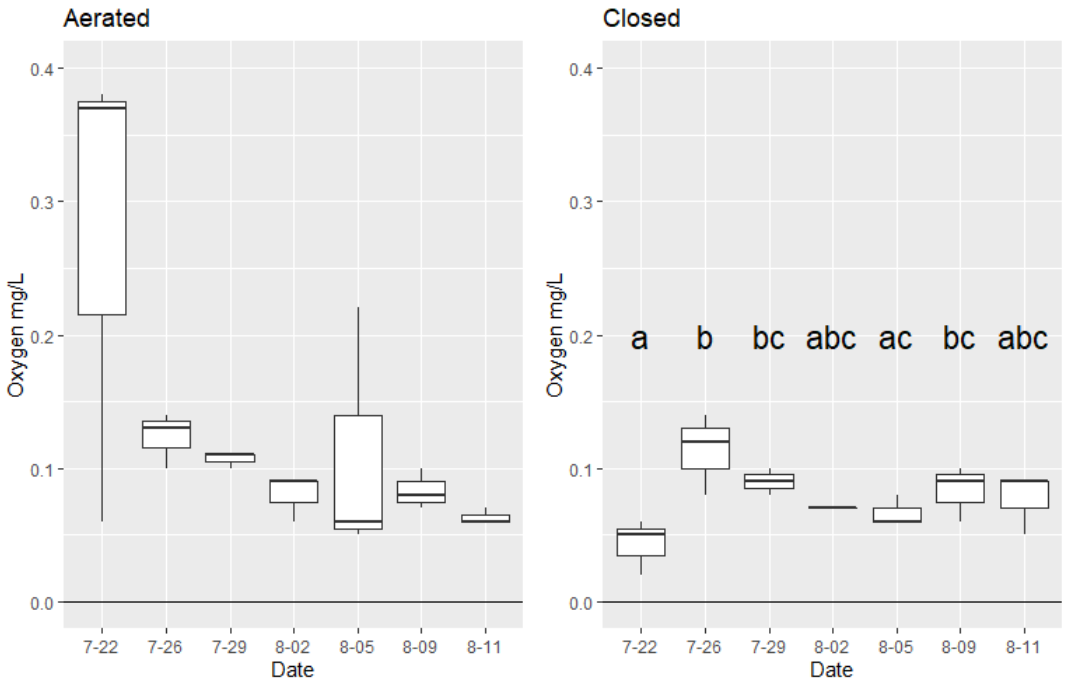

Figure 9. Dissolved oxygen concentrations both the aerated and closed wet conditions taken on each day of sampling during Experiment 2. Different letters show significant differences in dissolved oxygen between sampling days.

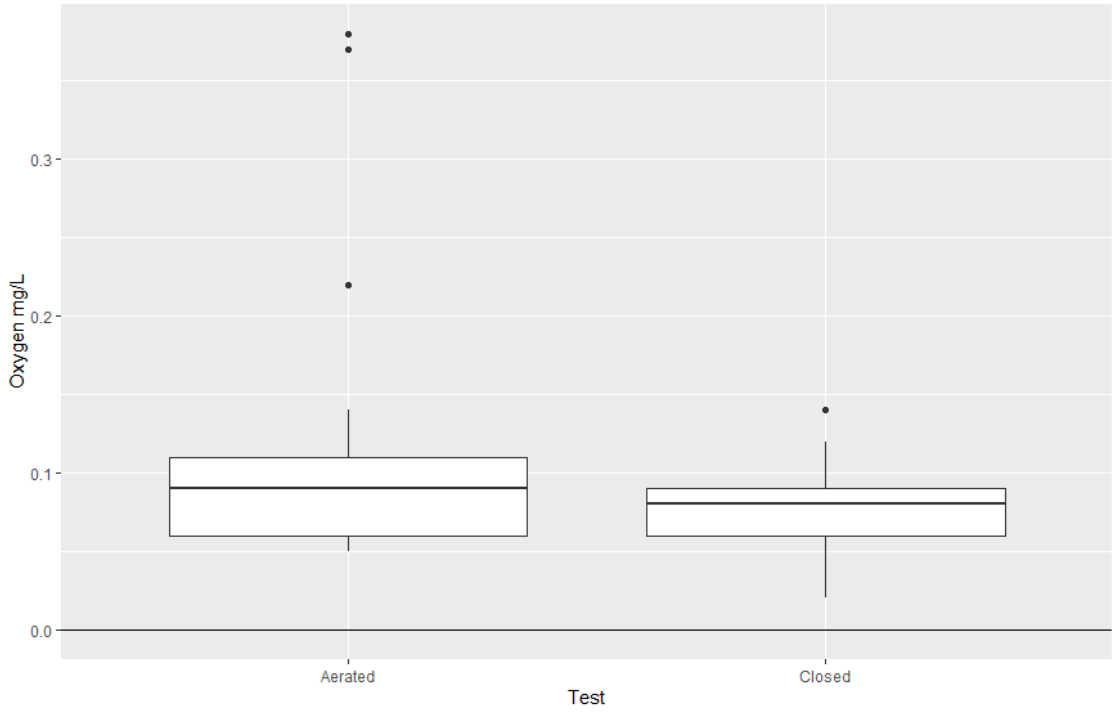

Figure 10. Dissolved oxygen concentrations in the different experimental conditions, from Experiment 2, compiled over every day of sampling.

Overall, CO_2 flux ranged from -18.4 to 163.8 µmol m^{-2} s^{-1} in Experiment 2. This range was greater than the fluxes measured in Experiment 1. In experiment 2, fluxes were significantly different per condition (Kruskal-Wallis, $p < 0.05$). CO_2 flux over time for each treatment is shown in figure 11, and CO_2 flux compared per treatment is shown in figure 13. CO_2 fluxes were lower in the wet conditions across both aeration treatments, with a maximum of 19.9 µmol $m^{-2}s^{-1}$ for wet closed and 8.1 µmol m^{-2} s^{-1} for wet aerated. The dry aerated treatment appeared to have larger fluxes, but this was mostly due to outliers. The dry closed treatment had a maximum of 163.8 µmol m^{-2} s^{-1} on August 9th, 2021. Negative fluxes were recorded in all treatments but dry closed, though the majority of fluxes were positive.

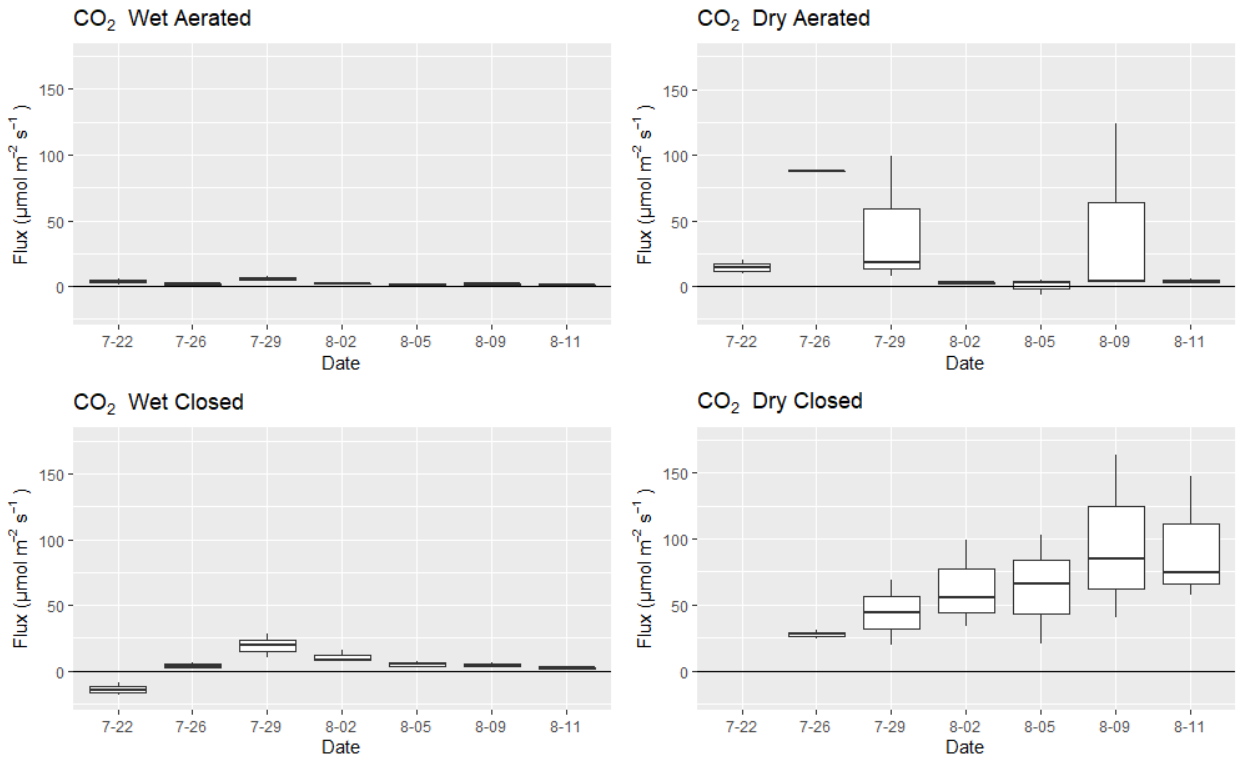

Figure 11. Carbon dioxide fluxes from the aeration experiments per each day of sampling.

CH_4 fluxes in Experiment 2 had a range from -1.5 to 6.2 nmol m^{-2} s^{-1}. The wet aerated condition appeared to have the highest instance of flux, 6.2 nmol m^{-2} s^{-1}, on August 5th. CH_4 fluxes were significantly different per condition (Kruskal-Wallis, $p < 0.05$), with the wet aerated

condition showing significantly higher fluxes than the dry closed condition. CH_4 flux over time is shown in figure 12, and CH_4 flux per treatment is shown in figure 13.

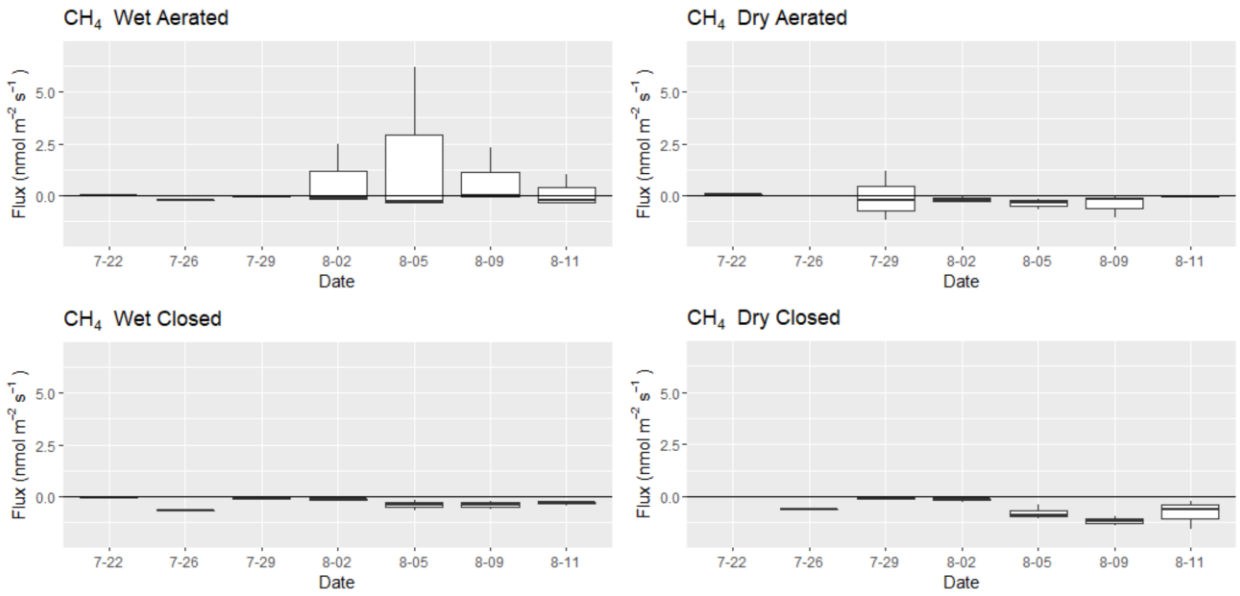

Figure 12. CH_4 fluxes from experiment 2 per conditions crossing seawater immersion and dry mesocosms, and aerated and closed mesocosms over each day of incubation.

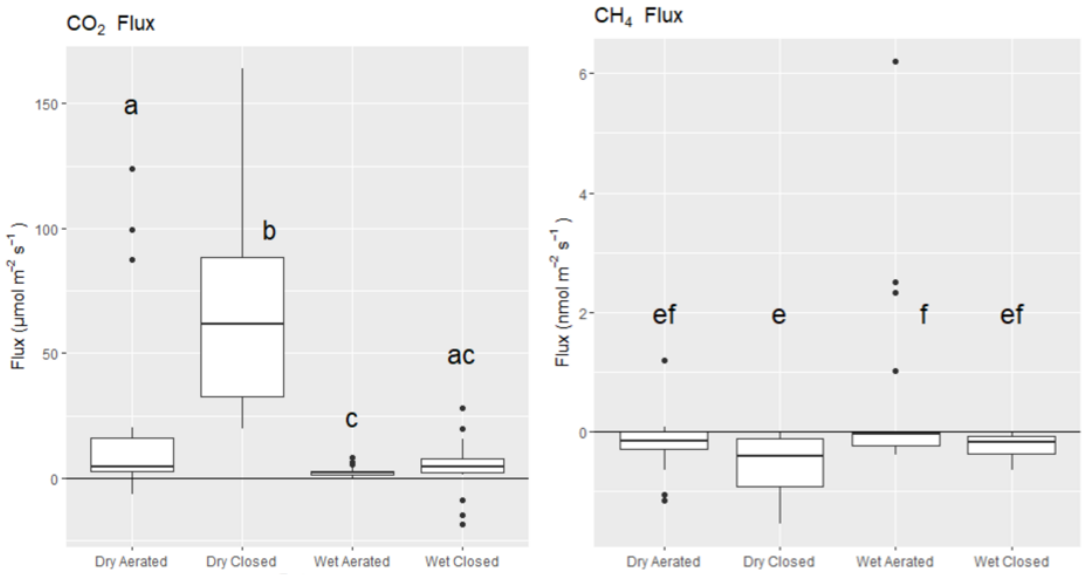

Figure 13. CO_2 and CH_4 fluxes from experiment 2, per conditions crossing seawater immersion and dry mesocosms, and aerated and closed mesocosms, compiled over each day of sampling. Different letters show significant differences in flux between tests.

Overall, TA ranged from 7046.1 µmol kg^{-1} to 72,422.0 µmol kg^{-1}. TA was found to be different over time in the aerated treatment (one-way repeated measures ANOVA, $p < 0.05$) and in the closed treatment (one-way repeated measures ANOVA, $p < 0.05$). TA per condition was not found to be significantly different (Wilcoxon rank sum test, $p = 0.49$, Figure 15). TA over time for each treatment can be seen in figure 14, and the comparison of TA between the treatments can be seen in figure 15.

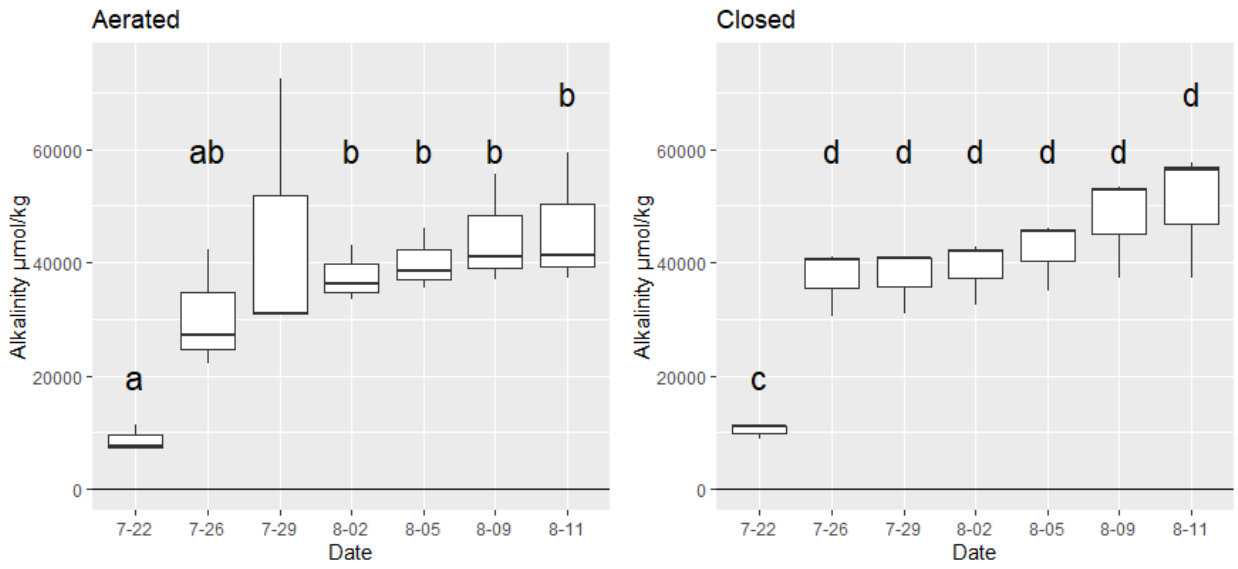

Figure 14. TA per each day of incubation for conditions of aerated and closed in experiment 2. Dates with significantly different TA within treatments are denoted by different letters.

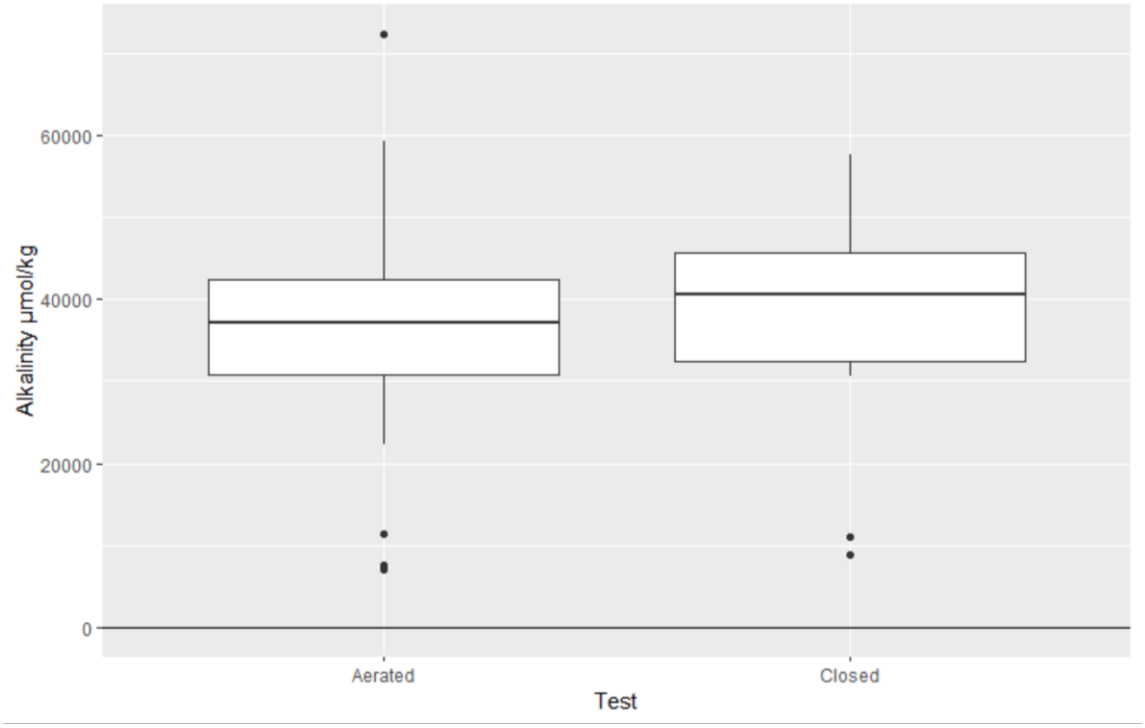

Figure 15. Comparison of TA between aerated and closed conditions in experiment 2, compiled over each day of sampling.

pH was found to change significantly over time in the aerated treatment (one-way repeated measures ANOVA, $p < 0.05$), but not in the closed treatment (repeated measures ANOVA, $p = 0.18$). pH between conditions was not found to be significantly different (Wilcoxon rank sum test, $p = 0.78$). pH data in aerated conditions started in a low pH, then became slightly higher for the rest of the experiment. pH over time for either condition can be seen in figure 16, and the comparison of pH between conditions can be seen in figure 17.

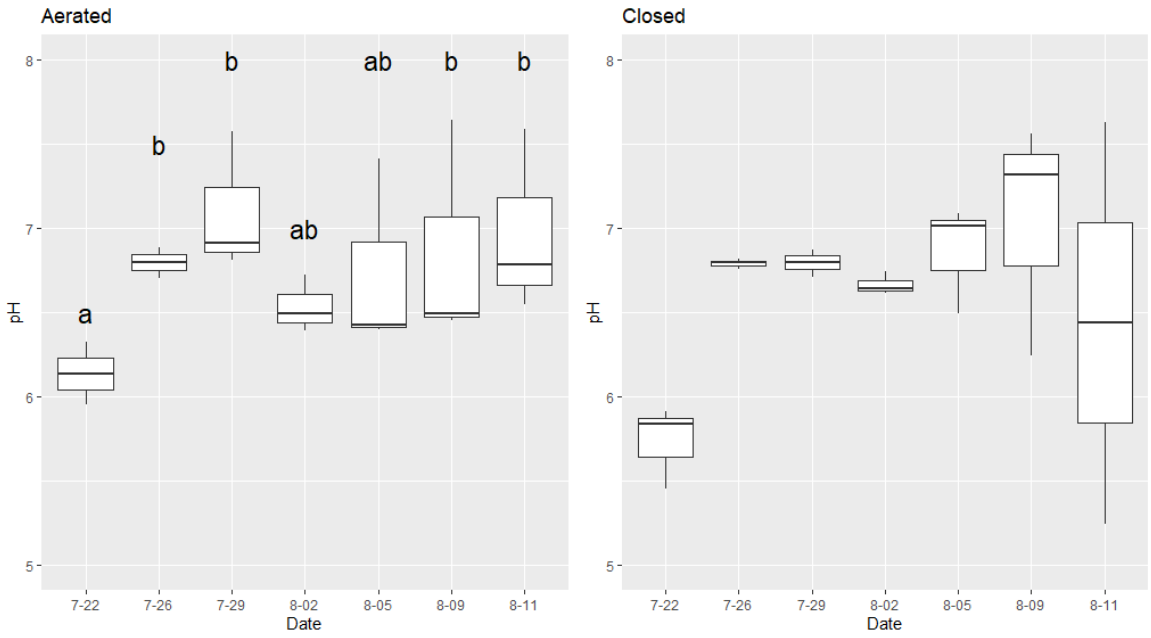

Figure 16. pH data over time for both the aerated and closed conditions, from experiment 2. Different letters show significant differences in pH between days.

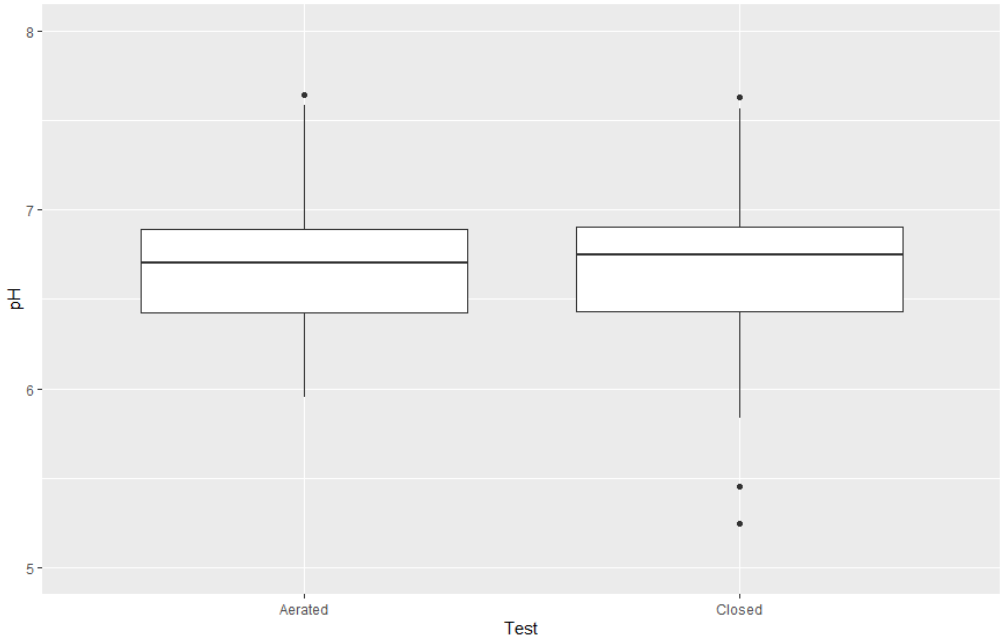

Figure 17. Comparison of pH between aerated and closed conditions, from experiment 2.

TA:DIC ratios were used to identify the biogeochemical process that led to increasing alkalinity in the seawater mesocosms (Figure 20). The slope of the correlation for both the aerated and closed experimental conditions were close to 1, which is the expected slope for decomposition driven by sulfate reduction (Table 1).

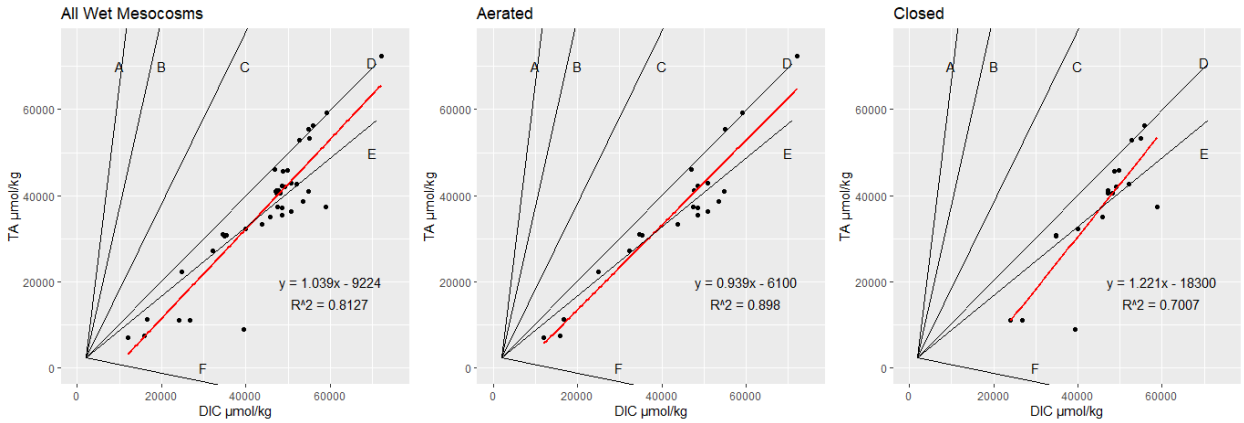

Figure 18. Correlations between TA and DIC in the seawater mesocosms in experiment 2. The red line indicates trend line, and black lines indicate stoichiometric relationships between TA and DIC as expected with iron reduction (A), manganese reduction (B), calcium carbonate dissolution (C), sulphate reduction (D), denitrification (E) and aerobic respiration (F).

Beach incubations

Beach incubations were completed on two separate days (September 9th and October 19th). Beach GHG fluxes from the September 9th sampling were calculated and reported in Figure 19. Since replicates were not done for September 9th incubations, data are reported as bar plots. Sand had low GHG flux overall (1.86 µmol $m^{-2}s^{-1}$ CO_2, 0.15 nmol $m^{-2}s^{-1}$ CH_4), and deep *Sargassum* had low CO_2 flux (5.06 µmol m^{-2} s^{-1}), While shallow *Sargassum* had the highest CO_2 flux (32.3 µmol m^{-2} s^{-1}). Dry, deep, and shallow *Sargassum* had similar CH_4 concentrations.

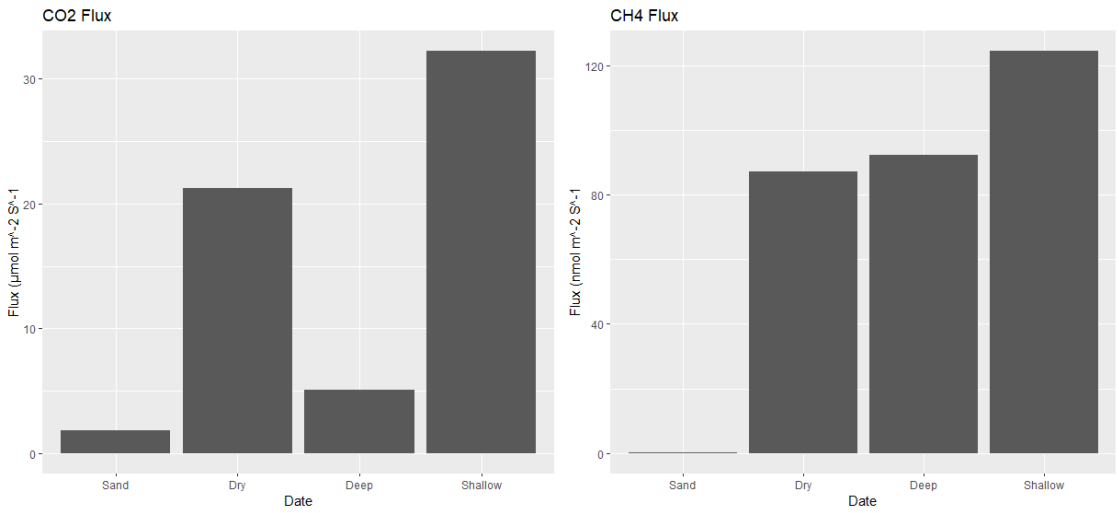

Figure 19. CO_2 and CH_4 fluxes from September beach incubations, in µmol/m^2s and nmol/ m^2s, respectively.

Beach GHG fluxes from the October 19th sampling were calculated and reported in Figure 20. October 19th incubations had three incubations of each type. Fluxes ranged from 9.69 to 466.11 µmol m^{-2} s^{-1} for CO_2 and from 1.08 to 703.20 nmol m^{-2} s^{-1} for CH_4. Although the sand GHG fluxes were much greater on October 19th than on September 9th, the shallow and deep *Sargassum* fluxes were not very different between the two days.

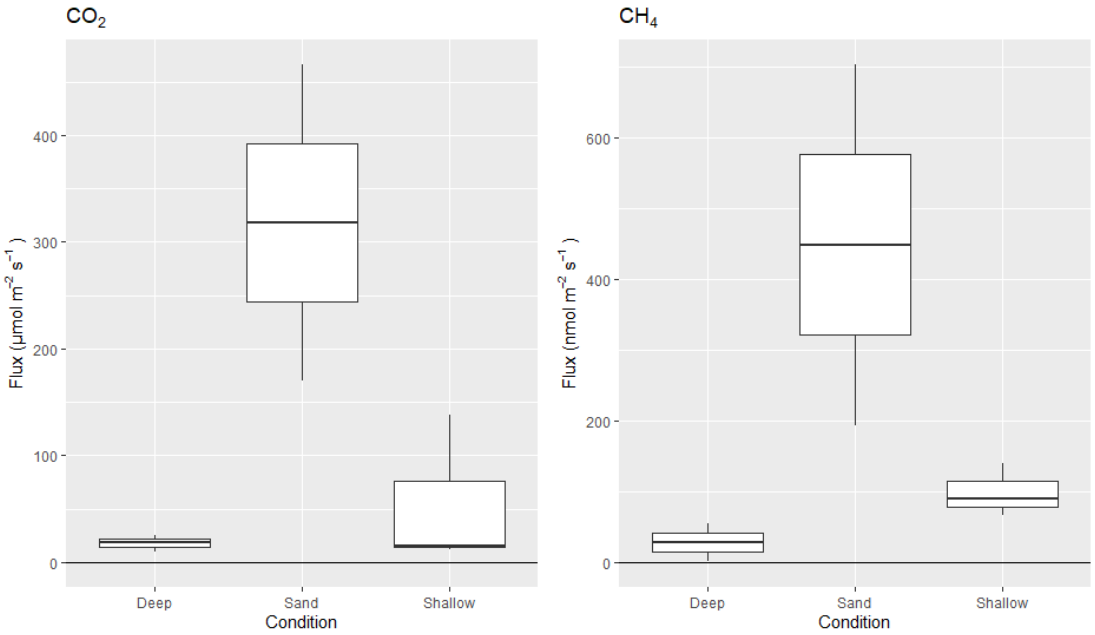

Figure 20. CO_2 and CH_4 fluxes from October beach incubations, in µmol/m^2s and nmol/ m^2s, respectively.

Discussion

In this study, CO_2 fluxes in decomposing *Sargassum* were not found to be significantly different between experimental conditions of dry, immersed in seawater and the tidal simulation. In experiment 2, although aerated and closed conditions were meant to cause oxygenated and anoxic conditions, dissolved oxygen was not significantly different between aerated and closed mesocosms. GHG fluxes in decomposing *Sargassum* were not found to be significantly different between the aerated and closed conditions, though there were significant differences between dry and immersed in this experiment. TA and pH were both not significantly different between aerated and closed mesocosms, but TA did change over time. Analysis of TA:DIC ratios revealed stoichiometry that best related to sulfate reduction occurring in the mesocosms over the duration of the experiment. Lastly, although beach incubations revealed higher CH_4 fluxes than those found in the mesocosms experiments, unpredictable sand GHG fluxes brought the accuracy of the beach data into question. The results present some interesting trends; however, it is important to note that experiments better mimicking the natural decay process should be conducted. These results provide some baseline GHG flux data that should spur interesting and important research into the carbon cycle of coastal wrack accumulations.

Although the tidal simulation was expected to cause higher CO_2 fluxes than the other treatments, CO_2 flux was not found to be different from the dry and immersed treatments. Tidal action has been found to be a driver of macroalgal decomposition on beaches, so these results may be due to the limitations of the mesocosm design (Erk et al. 2020, Perkins et al. 2022). This mesocosm design attempted to simulate cycles of desiccation and inundation, though due to the closed design of the mesocosm it is possible that proper desiccation was not achieved. During the experiment, when the tidal mesocosms were opened for incubation, the *Sargassum* wrack was never dry so the conditions may never have deviated very far from the conditions of the mesocosms in which *Sargassum* was immersed in seawater. However, in the immersion treatment the *Sargassum* was submerged or floating, while in the tidal simulation the Sargassum was suspended over the seawater in the bottom of the mesocosm. Another limitation of this mesocosm experiment was the lack of inclusion of beach sediment, potentially meaning these experiments lacked the microbial communities native to beaches that drive decomposition (Perkins et al. 2022). In addition to microbial communities, porewater filtering can lead to accelerated mineralization of organic matter (Santos et al. 2012), so the lack of sediment may

have impacted the GHG fluxes measured here. In addition, the lack of a flow-through seawater system may have led to the build-up of decomposition products which could have impacted GHG fluxes. This can be seen in the build-up of alkalinity (Figure 14), and although nitrates and phosphates were not tested for, these are seen to increase in coastal waters following decomposition of *Sargassum* (van Tussenbroek et al. 2017). Sandy beaches covered in macroalgae wrack are characterized by an export of excess reduced compounds (Erk et al. 2020), so a system that does not allow for the removal of these products may not properly simulate natural decomposition processes. A more comprehensive mesocosm design might look more like the mesocosms used in Perkins et al. (2022), which included columns of beach sediment to study porewater dynamics and a flow-through seawater system. The initial activity found in the dry treatments may have been due to remaining moisture from the beginning of the experiment. The lowering flux over time suggests wrack releases less CO_2 as it dries over time, and this best simulates wrack that sits on beaches above the high-tide line. It has been suggested that macroalgal wrack high on beaches can serve as a temporary sink of carbon, until it is disturbed by abnormally high tides or storms (Rodil et al. 2018).

In experiment 1, the presence of methanogenesis was not supported by the collected CH_4 data. CH_4 flux was not calculated or reported in experiment 1 because the majority of the incubations did not return CH_4 emission rates with R^2 greater than 0.9. Since all mesocosms in experiment 1 were aerated, this could reflect that the *Sargassum* wrack did not provide the anaerobic environment necessary for methanogenesis (Erk et al. 2020). However, this apparent lack of methanogenesis could be explained by other anaerobic reactions that compete for the same reactants. Sulfate reducers compete with methanogens, as both require acetate and hydrogen as reactants (Sansone & Martens 1982, Erk et al. 2020). It is conventionally thought that the high sulfate concentration of seawater means that these reactions tend to occur in sequence, with methanogenesis not happening until sulfate has been depleted (Froelich et al. 1979). In some cases, methanogenesis and sulfate reduction have been found to co-occur in marine sediments, although methane production is generally much lower in the presence of sulfate reducing bacteria (Sela-Adler et al. 2017). Another reason for low GHG fluxes from these mesocosms may have been a film that formed on the surface of wet mesocosms (Fig. 1). This film may have limited gas exchange into the bottom of the mesocosm and limited the *Sargassum's* access to oxygen as the wrack sunk below the surface over the course of the

experiment. Since there were no methods of bacterial or fungal identification in this study, it is unknown what specifically caused this film to form.

Analysis of dissolved oxygen concentrations in experiment 2 confirmed that aeration of the mesocosm does not affect the oxygen concentration of the seawater after the first few days of the experiment (Figure 9, 10). Hypoxic conditions occur under 5 mg/L of oxygen (Killgore & Hoover 2001), and the average oxygen concentration for all mesocosms during experiment 2 was under 0.1 mg/L. CO_2 fluxes in experiment 2 were not found to be significantly affected by the sampling date, which means CO_2 fluxes did not change over time. Despite this lack of change over time, all levels of treatment were found to significantly affect CO_2 flux. Similarly to fluxes found in Experiment 1, Experiment 2 reported low CO_2 fluxes in mesocosms that included seawater immersion (-9.2:8.3 μmol $m^{-2}s^{-1}$ for Ex. 1; -14.7:27.9 μmol m^{-2} s^{-1} for Ex. 2). In comparison to other studies that investigate CO_2 flux in macroalgae wrack, average fluxes from the wet experiments were closest to past fluxes recorded to macroalgae, while average fluxes from the dry experiments were greater (Table 2). The same bacterial/fungal film that occurred in experiment 1 also occurred in experiment 2, which may have inhibited the exchange of GHGs across the air-water interface. Dry experimental mesocosms reported greater CO_2 fluxes than the seawater mesocosms (Fig. 11), which is counter to the expectation that the aerated mesocosms would show greater aerobic respiration. This reflects a failure in the aeration design to create differently oxygenated conditions. Dry mesocosms most likely reached higher CO_2 fluxes because *Sargassum* in the seawater treatments were almost fully submerged by the end of the testing period, with little contact with the air space that was being aerated.

The majority of CH_4 fluxes in experiment 2 were negative, indicating net uptake of CH_4 by the mesocosms. This was unexpected, as past studies that investigated CH_4 fluxes in blue carbon ecosystems reported positive fluxes (Table 2). However, this may be a consequence of attempting to simulate beach conditions in a mesocosm. Since mesocosms had to be brought to ambient atmosphere conditions before the incubations could start, it is possible that these negative fluxes were caused by oxidation of CH_4 as microbes in the wrack became exposed to oxygen. CH_4 oxidation can be caused by methanotrophic bacteria, which are common in association with marine macrophytes (Sorrel et al 2002, Brian Jones et al. 2003). However, this conclusion is speculative and assumes a rapid change in bacterial activity during incubations. Another lack of CH_4 fluxes may have been caused by high rates of sulfate reduction and

competition between sulfate reducers and methanogens for organic matter (Sela-Adler et al. 2017).

The presence of sulfur reduction could explain the lack of observed methanogenesis as methanogenic bacteria compete with sulfur reducers for hydrogen and acetate in anaerobic environments. Methanogenesis in *Sargassum* may not become a prominent biogeochemical process until reducible sulfate has been depleted from the wrack (Sasone & Martens 1982, Erk et al 2020). Sulfur reduction is very common in macroalgal decomposition (Erk et al 2020, Perkins et al. 2022) and especially in *Sargassum* decomposition (Resiere et al. 2018, Gray et al. 2021), largely due to the high concentration of sulfate in seawater. In this study, DIC and TA data from the wet incubations were used to determine the relative abundance of different biogeochemical pathways (Figure 19). This analysis demonstrated that sulfate reduction was likely an important biogeochemical pathway during the wet incubations. Since water samples were not taken from the dry mesocosms, it is unknown whether this also explains low CH_4 fluxes in the dry conditions. Interestingly, positive CH_4 fluxes were detected in the beach data (Figure 17, 18). Since this data was taken late in the season and on highly degraded *Sargassum*, reducible sulfate may have been depleted, allowing for methanogens to become dominant. In the macroalgae decomposition experiment by Perkins et al (2022), CH_4 production was not significant until the 25th day, and was ongoing until the end of the experiment at 60 days. In the present study, mesocosm experiments were only carried out for 21 days. An experiment with a longer duration could be expected to show shifts towards different anaerobic pathways (Table 1).

Total alkalinity in the mesocosms increased from ca. 10,000 µmol kg^{-1} to ca. 40,000 µmol kg^{-1} over the first few days of Experiment 2. For reference, normal seawater TA is ca. 2368.9 µmol kg^{-1} (Rangel 2021). In Experiment 2, the mean TA for both aerated and closed conditions (ca. 40,000 µmol kg^{-1}) was almost seventeen times normal seawater TA (Figure 15). This was most likely caused by the anaerobic decomposition of the wrack, most notably sulfate reduction, which increases TA of seawater (Sippo et al. 2016). All seawater mesocosms had low oxygen concentrations (Figure 9), which would allow for anaerobic decomposition and explain the large increase in alkalinity. Since mesocosms in this experiment did not have a flow-through design, the TA concentration would not be expected to decrease without any changes in the chemical conditions of the mesocosms. Perkins et al. (2022) recorded an increase in TA by the third day of their experiment, but this condition decreased over the course of the experiment. A

similar decrease in TA production was seen in the present study, as TA concentrations appeared to plateau later in the experiment, though it is unknown whether this was caused by a natural decrease in TA-producing reactions, or by the buildup of decomposition products.

This TA production could serve as another pathway of carbon sequestration. When 0.5 moles of sulfate are reduced, the reaction produces one mole of TA and one mole of DIC (Table 1), trapping carbon as TA. The hydrogen sulfide (HS^-) that is produced in this reaction can be reoxidized, which reverses this reaction and consumes TA (Moeslund et al. 1994). In marine sediments, if the sulfide is precipitated as total reduced sulfur the reaction does not reverse and carbon is stored as alkalinity in the long term (Moeslund et al. 1994, Thomas et al. 2009). Precipitation of sulfide occurs as iron reacts with HS^-, producing either iron monosulfide (FeS) or pyrite (FeS_2) and storing it long term in the sediment (Kristensen et al. 2000, Thomas et al. 2009). In conditions where the oxygenated sediment layer is thin, H_2S gas may also be released into the atmosphere, where it cannot be oxidized back to sulfate (Kristensen et al. 2000). Since sulfate reduction can sequester carbon if it is not reoxidized, evidence of sulfate reduction outcompeting methanogenesis in *Sargassum* decomposition suggests that this decomposition may serve as an additional sink of blue carbon. This study demonstrated that *Sargassum* decomposition drastically increased seawater alkalinity (Figure 14) and was driven by sulfate reduction (Figure 22). However, to fully understand this contribution to carbon sequestration, more data on CO_2 and CH_4 emission must be gathered to understand whether the alkalinity production significantly offsets GHG emission over the course of decomposition.

pH data was similar to TA data in that it was not significantly different between the aerated and closed conditions (Figure 17). This was presumably for similar reasons as to why this occurred with TA. Similar to the TA data, initial pH conditions were low (Figure 16), before increasing to between 6.5-7 for the rest of the study. The initial low pH was likely caused by initially high oxygen concentrations, allowing for aerobic respiration, which lowers both pH and TA. As oxygen concentrations decreased, aerobic respiration would also have decreased. However, this explanation is not supported by CO_2 flux data (Figure 11), which does not show an initially high CO_2 flux for either aerated or closed seawater conditions. This may be due to the nature of how this activity was recorded: CO_2 flux was not recorded until 20 hours after the beginning of the mesocosm experiment, so an initial spike of aerobic decomposition may have

been missed. It could also be that the seawater in the mesocosm was absorbing the majority of the CO_2 as DIC.

The purpose of the beach incubations in this study was to compare the mesocosm results to actual environmental conditions. The location where beach incubations were done, the northern end of the Dr. Von D. Mizell-Eula Johnson State Park beach, concentrates the stranding of *Sargassum* with large stone breakwaters. Over the course of the *Sargassum* season (April-August), large piles of *Sargassum* accumulated in this area (Figure 4). Beach incubations were done late in the *Sargassum* stranding season. The September incubations (Figure 20) showed strong fluxes of both CO_2 and CH_4 from dried piles of *Sargassum* and both shallow and deep piles of wet *Sargassum*, but not from the control sand patches. It was assumed that dry *Sargassum* patches would be less microbially active, but they had greater CO_2 flux than the deep *Sargassum* patches. It was also not expected that shallow *Sargassum* patches would have greater fluxes of both GHGs than deep *Sargassum* patches. Although deep patches had more seawater inundation and greater algal mass than the dry patches, it may be that mixing with sediments is more important for decomposition. Other studies that investigated decomposition of wrack on beaches (Erk et al. 2020, Perkins 2022) incorporated sediment depth into their experimental design. Perkins et al. (2022) specifically found that different biogeochemical processes important to wrack decomposition only occur at deeper sediment depths. Oscillating water tables, such as those found on a beach, drive microbial activity in soil (Rezanezhad et al. 2014), and buried wrack that is subject to these diurnal water table changes may have higher GHG fluxes than wrack that are only partially submerged while on the surface. It was observed that the beach used in this study had large amounts of buried *Sargassum* under the surface of the sand, and the experimental design of the incubations did not allow for quantification of this buried wrack. The dry sand incubations, which were not done in areas with this buried *Sargassum*, did not show much GHG flux, as was expected.

Beach incubations done in October had unexpectantly high GHG fluxes from dry sand, which was meant to be a control. In October incubations, three replicates of each type of *Sargassum* and beach sand were incubated for more reliable results. However, two out of three sand patches had much greater GHG flux than the shallow and deep wet *Sargassum* patches, while the third sand patch was removed from the data for having a low R^2 for slope of gas concentration. Once again, shallow wet *Sargassum* had higher GHG fluxes than deep wet

Sargassum. Unexpected fluxes from the bare sand may have been caused by the tide pushing groundwater up into the beach face (Perkins 2022). Wrack incubations on this day were started at slack low tide while sand incubations were done later than wrack incubations, and the tide was observably starting to come in. Rising tides can cause changes in microbial activity in sandy beaches (Hubas et al. 2006, Rezanezhad et al. 2014), which may be the reason why the control sand patches had relatively high GHG fluxes. It is possible that the sites that the wrack was resting on would also have this high flux, if not for the degraded *Sargassum* resting on top of it. Despite unexpected sand fluxes, the *Sargassum* fluxes were higher than those found in the mesocosm experiments. As stated earlier, this may have been due to the significance of sand and natural bacterial communities in wrack decomposition, as sand was not present in the mesocosms. Another difference may have been temperature. Macroalgal wrack exposed to high temperatures on sandy beaches are known to have higher CO_2 fluxes (Lastra et al. 2018). Mesocosms in the present study were housed in shade to reduce evaporation of seawater within buckets. Since mesocosms were shaded, they did not experience the direct sunlight that beach wrack does on a normal day.

Table 2. CO_2 and CH_4 fluxes from blue carbon ecosystems and macroalgal wrack, from previous studies and this current study.

Material	Location	CO_2 (µmol m^{-2} s^{-1})	CH_4 (nmol m^{-2} s^{-1})	Citation
Macroalgae (*Saccorhiza polyschides*)	América beach, Spain	3.4 ± 0.6	--	Rodil et al. 2019
Macroalgae (*Undaria pinnatifida*)	América beach, Spain	6.5 ± 0.9	--	
Macroalgae (*Cystoseira baccata*)	América beach, Spain	1.4 ± 0.2	--	
Macroalgae (*Sargassum muticum*)	América beach, Spain	2.7 ± 0.6	--	
Mangrove adjacent waters, wet season	Burdekin River, Australia	68.81	3.48 ± 0.10	Rosentreter et al. 2018
Mangrove adjacent waters, dry season	Burdekin River, Australia	54.53	1.25 ± 0.05	
Mangrove adjacent waters, wet season	Fitzroy River, Australia	58	12.15 ± 0.54	
Mangrove adjacent waters, dry season	Fitzroy River, Australia	20.31	1.12 ± 0.08	
Mangrove adjacent waters, wet season	Johnstone River, Australia	--	9.56	
Mangrove adjacent waters, dry season	Johnstone River, Australia	17.89	5.71 ± 0.11	
Mangrove adjacent waters	Nagada Creek, Papua New Guinea	0.50 ± 0.38	--	Borges et al. 2003
Mangrove adjacent waters	Gaderu Creek, India	0.65 ± 1.17	--	
Mangrove adjacent waters	Norman's Pond, Bahamas	0.16 ± 0.10	--	
Seagrass bed (*Thalassodendron ciliatum*)	Red Sea, Audi Arabia	--	0.04	Garcias-Bonet & Duarte 2017
Seagrass bed (*Halophila decipiens*)	Red Sea, Audi Arabia	--	0.08	
Seagrass bed (*Enhalus acoroides*)	Red Sea, Audi Arabia	--	1.11	
pelagic *Sargassum* wrack	Ft Lauderdale	4.02 ± 0.52	--	This study, experiment 1 wet
pelagic *Sargassum* wrack	Ft Lauderdale	10.63 ± 3.02	--	This study, experiment 1 dry
pelagic *Sargassum* wrack	Ft Lauderdale	4.58 ± 1.16	--	This study, experiment 1 tidal
pelagic *Sargassum* wrack	Ft Lauderdale	21.52 ± 8.62	-0.19 ± 0.13	This study, experiment 2 dry aerated
pelagic *Sargassum* wrack	Ft Lauderdale	68.04 ± 10.83	-0.57 ± 0.13	This study, experiment 2 dry closed
pelagic *Sargassum* wrack	Ft Lauderdale	2.53 ± 0.47	0.55 ± 0.39	This study, experiment 2 wet aerated
pelagic *Sargassum* wrack	Ft Lauderdale	4.52 ± 2.35	-0.25 ± 0.05	This study, experiment 2 wet closed

Conclusions

Sargassum strandings in the Caribbean and Gulf of Mexico have becoming more common and greater in size since the formation of the great Atlantic *Sargassum* belt in 2011. Health and ecological consequences of these events have been observed in past studies (Resiere et al. 2018, Gray et al. 2021). However, *Sargassum's* role as a blue carbon sink is still unknown. The goal of this study was to examine the potential GHG fluxes and carbonate chemistry changes associated with *Sargassum* standings on a South Florida beach, and this was done with the use of mesocosms to simulate how different conditions may affect the carbon cycle associated with *Sargassum*. Overall, a more sophisticated mesocosm setup that mimics natural processes is needed to better determine fluxes of GHGs. Although CO_2 flux was detected, it is unclear how that flux may change over time. Methanogenesis may have been inhibited by sulfate reduction, which was detected through analysis of TA and DIC. Sulphate reduction in stranded wrack may also add to the blue carbon potential of *Sargassum*, as this reaction adds DIC to seawater as alkalinity. Methanogenesis most likely occurs later in the degradation process as sulfate is depleted from wrack and methanogens do not have to compete for reactants. Since many biogeochemical processes are inherent to marine sediments, future studies should include sand in mesocosm design or directly study *Sargassum* strandings as they decompose on beaches. Overall, methane fluxes were detected from naturally degrading *Sargassum*, which indicates this source of a highly potent GHG could offset any atmospheric CO_2 that is buried by sinking *Sargassum*. Future studies and *Sargassum* management policies should take the production of GHGs by decomposition pathways in stranded *Sargassum* mats into consideration.

Literature Cited

Archer, D. (2005). Fate of fossil fuel CO_2 in geologic time. *Journal of Geophysical Research, 110*(C9)

Baker, P., Minzlaff, U., Schoenle, A., Schwabe, E., Hohlfeld, M., Jeuck, A., Brenke, N., Prausse, D., Rothenbeck, M., Brix, S., Frutos, I., Jörger, K. M., Neusser, T. P., Koppelmann, R., Devey, C., Brandt, A., & Arndt, H. (2018). Potential contribution of surface-dwelling Sargassum algae to deep-sea ecosystems in the southern North Atlantic. *Deep Sea Research Part II: Topical Studies in Oceanography*, *148*, 21-34.

Borges, A. V. (2003). Atmospheric CO_2 flux from mangrove surrounding waters. *Geophysical Research Letters*, *30*(11).

Boucher, O., Friedlingstein, P., Collins, B., & Shine, K. P. (2009). The indirect global warming potential and global temperature change potential due to methane oxidation. *Environmental Research Letters*, *4*(4).

Brian Jones, W., Cifuentes, L.A., Kaldy, J.E. (2003). Stable carbon isotope evidence for coupling between sedimentary bacteria and seagrasses in a sub-tropical lagoon. *Mar Ecol Prog Ser*, *255*, 15-25.

Cyronak, T., Santos, I. R., McMahon, A., & Eyre, B. D. (2013). Carbon cycling hysteresis in permeable carbonate sands over a diel cycle: Implications for ocean acidification. *Limnology and Oceanography*, *58*(1), 131-143.

Dickson, A. G., & Millero, F. J. (1987). A comparison of the equilibrium constants for the dissociation of carbonic acid in seawater media. *Deep Sea Research 34*(10), 1733-2743.

Dickson, A.G., Sabine, C.L. and Christian, J.R. (Eds.) (2007). Guide to Best Practices for Ocean CO_2 Measurements. PICES Special Publication 3, 191 pp.

Duarte, C. M., & Cebrián, J. (1996). The fate of marine autotrophic production. *Limnology and Oceanography*, *41*(8), 1758-1766.

Duarte, C.M., Middelburg, J. J., Caraco, N. (2005). Major role of marine Vegetation on the oceanic carbon cycle. *Biogeosciences*, *2*, 1-8.

Erk, M. R., Meier, D. V., Ferdelman, T., Harder, J., Bussmann, I., & Beer, D. (2020). Kelp deposition changes mineralization pathways and microbial communities in a sandy beach. *Limnology and Oceanography*, *65*(12), 3066-3084.

Filbee-Dexter, K., & Wernberg, T. (2020). Substantial blue carbon in overlooked Australian kelp forests. *Sci Rep*, *10*(1), 12341.

Froelich, P.N., Klinkhammer, G.P., Bender, M.L., Luedtke, N.A., Heath, G.R., Cullen, D., Dauphin, P. (1979). Early oxidation of organic matter in pelagic sediments of the eastern equatorial Atlantic: suboxic diagenesis. *geochemical Journal et Cosmochimica Acta*, 43, 1075-1090.

Fuglestvedt, J.S., Isakseb, I.S.A., & Wang, W.C. (1996). Estimates of Indirect Global Warming Potentials for CH_4, CO and NO_x. *Climatic Change*, *34*, 405-437.

Garcias-Bonet, N., & Duarte, C. M. (2017). Methane Production by Seagrass Ecosystems in the Red Sea. *Frontiers in Marine Science, 4*.

Gouvea, L. P., Assis, J., Gurgel, C. F. D., Serrao, E. A., Silveira, T. C. L., Santos, R., Duarte, C. M., Peres, L. M. C., Carvalho, V. F., Batista, M., Bastos, E., Sissini, M. N., & Horta, P. A. (2020). Golden carbon of Sargassum forests revealed as an opportunity for climate change mitigation. *Sci Total Environ*, *729*, 138745.

Gray, L. A., Bisonó León, A. G., Rojas, F. E., Veroneau, S. S., & Slocum, A. H. (2021). Caribbean-Wide, Negative Emissions Solution to Sargassum spp. Low-Cost Collection Device and Sustainable Disposal Method. *Phycology*, *1*(1), 49-75.

Hernández, W. J., Morell, J. M., & Armstrong, R. A. (2021). Using high-resolution satellite imagery to assess the impact of Sargassum inundation on coastal areas. *Remote Sensing Letters*, *13*(1), 24-34.

Hu, C., Wang, M., Lapointe, B. E., Brewton, R. A., & Hernandez, F. J. (2021). On the Atlantic pelagic Sargassum's role in carbon fixation and sequestration. *Science of The Total Environment, 781*.

Hubas, C., Lamy, D., Artigas, L. F., & Davoult, D. (2006). Seasonal variability of intertidal bacterial metabolism and growth efficiency in an exposed sandy beach during low tide. *Marine Biology*, *151*(1), 41-52.

Hyun, J.-H., Kim, S.-H., Mok, J.-S., Cho, H., Lee, T., Vandieken, V., & Thamdrup, B. (2017). Manganese and iron reduction dominate organic carbon oxidation in surface sediments of the deep Ulleung Basin, East Sea. *Biogeosciences*, *14*(4), 941-958.

Itoh, H., Aoki, M. N., Tsuchiya, Y., Sato, T., Shinagawa, H., Komatsu, T., Mikami, A., & Hama, T. (2007). Fate of organic matter in faecal pellets egested by epifaunal mesograzers in a Sargassum forest and implications for biogeochemical cycling. *Marine Ecology Progress Series, 352*, 101-112

IPCC, 2021: Climate Change 2021: The Physical Science Basis. Contribution of Working Group I to the Sixth Assessment Report of the Intergovernmental Panel on Climate Change [Masson-Delmotte, V., P. Zhai, A. Pirani, S.L. Connors, C. Péan, S. Berger, N. Caud, Y. Chen, L. Goldfarb, M.I. Gomis, M. Huang, K. Leitzell, E. Lonnoy, J.B.R. Matthews,

T.K. Maycock, T. Waterfield, O. Yelekçi, R. Yu, and B. Zhou (eds.)]. Cambridge University Press. In Press.

Josselyn, M.N., Cailliet G. M., Niesen, T.M., Cowen, R., Hurley A.C., Connor, J., Hawes, S., (1982). Composition, export and faunal utilization of drift in the salt river submarine canyon. *Estuarine, Coastal and Shelf Science 17*, 447-465.

Killgore, K.J., Hoover, J.J. (2001). Effects of Hypoxia on Fish Assemblages in a Vegetated Waterbody. *J. Aquat. Plant Manage*., *39*, 40-44.

Kokubu, Y., Rothausler, E., Filippi, J. B., Durieux, E. D. H., & Komatsu, T. (2019). Revealing the deposition of macrophytes transported offshore: Evidence of their long-distance dispersal and seasonal aggregation to the deep sea. *Sci Rep, 9*(1), 4331.

Krause-Jensen, D., & Duarte, C. M. (2016). Substantial role of macroalgae in marine carbon sequestration. *Nature Geoscience*, *9*(10), 737-742.

Kristensen E., Bodenbender J., Jensen M. H., Rennenberg H., Jensen K. M., (2000). Sulfur cycling of intertidal Wadden Sea sediments (Konigshafen, Island of Sylt, Germany): sulfate reduction and sulfur gas emission. *Journal of Sea Research, 43*, 93-104.

Krumins, V., Gehlen, M., Arndt, S., Van Cappellen, P., & Regnier, P. (2013). Dissolved inorganic carbon and alkalinity fluxes from coastal marine sediments: model estimates for different shelf environments and sensitivity to global change. *Biogeosciences, 10*(1), 371-398.

Krumhansl, K. A., & Scheibling, R. E. (2012). Production and fate of kelp detritus. *Marine Ecology Progress Series*, *467*, 281-302

Kwan, V., Fong, J., Ng, C. S. L., & Huang, D. (2022). Temporal and spatial dynamics of tropical macroalgal contributions to blue carbon. *Sci Total Environ, 828*, 154369.

Lapointe, B. E., Brewton, R. A., Herren, L. W., Wang, M., Hu, C., McGillicuddy, D. J., Lindell, S., Hernandez, F. J., & Morton, P. L. (2021). Nutrient content and stoichiometry of pelagic Sargassum reflects increasing nitrogen availability in the Atlantic Basin. *Nature Communications, 12*(1)

Lastra, M., Lopez, J., & Rodil, I. F. (2018). Warming intensify CO_2 flux and nutrient release from algal wrack subsidies on sandy beaches. *Glob Chang Biol, 24*(8), 3766-3779.

Lawson, G. S., Tyler, P. A., Young C.M., (1993). Attraction of deep-sea amphipods to macrophyte food falls. *J. Exp. Mar. Biol. Ecol., 163*, 33-39.

Lechtenfeld, O. J., Kattner, G., Flerus, R., McCallister, S. L., Schmitt-Kopplin, P., & Koch, B. P. (2014). Molecular transformation and degradation of refractory dissolved organic matter in the Atlantic and Southern Ocean. *Geochimica et Cosmochimica Acta, 126*, 321-337.

Li, Y., Fu, X., Duan, D., Liu, X., Xu, J., & Gao, X. (2017). Extraction and Identification of Phlorotannins from the Brown Alga, Sargassum fusiforme (Harvey) Setchell. *Mar Drugs, 15*(2).

Martin, L. M., Taylor, M., Huston, G., Goodwin, D. S., Schell, J. M., & Siuda, A. N. S. (2021). Pelagic Sargassum morphotypes support different rafting motile epifauna communities. *Marine Biology, 168*(7).

Maurer, A. S., De Neef, E., & Stapleton, S. (2015). Sargassum accumulation may spell trouble for nesting sea turtles. *Frontiers in Ecology and the Environment, 13*(7), 394-395.

Mikhaylov, A., Moiseev, N., Aleshin, K., & Burkhardt, T. (2020). Global climate change and greenhouse effect. *Entrepreneurship and Sustainability Issues, 7*(4), 2897-2913.

Milledge, J. J., Maneein, S., Arribas López, E., & Bartlett, D. (2020). Sargassum Inundations in Turks and Caicos: Methane Potential and Proximate, Ultimate, Lipid, Amino Acid, Metal and Metalloid Analyses. *Energies, 13*(6).

Moeslund, L, Thamdrup, B., Jorgenson, B.B., (1994). Sulfur and iron cycling in a coastal sediment: Radiotracer studies and seasonal dynamics. *Biogeochemistry, 27*, 129-152.

Nelleman, C., Corcoran, E., Duarte, C. M., Valdes, L., Deyoung, C., Fonseca, L., Grimsditch, G. (2009). *Blue Carbon The role of healthy oceans in binding carbon*. Birkeland Trykkeri AS, Norway.

Paraguay-Delgado, F., Carreno-Gallardo, C., Estrada-Guel, I., Zabala-Arceo, A., Martinez-Rodriguez, H. A., & Lardizabal-Gutierrez, D. (2020). Pelagic Sargassum spp. capture CO_2 and produce calcite. *Environ Sci Pollut Res Int, 27*(20), 25794-25800.

Pendleton, L., Donato, D. C., Murray, B. C., Crooks, S., Jenkins, W. A., Sifleet, S., Craft, C., Fourqurean, J. W., Kauffman, J. B., Marba, N., Megonigal, P., Pidgeon, E., Herr, D., Gordon, D., & Baldera, A. (2012). Estimating global "blue carbon" emissions from conversion and degradation of vegetated coastal ecosystems. *PLoS One, 7*(9), e43542.

Perkins, A. K., Santos, I. R., Rose, A. L., Schulz, K. G., Grossart, H.-P., Eyre, B. D., Kelaher, B. P., & Oakes, J. M. (2022). Production of dissolved carbon and alkalinity during macroalgal wrack degradation on beaches: a mesocosm experiment with implications for blue carbon. *Biogeochemistry*.

Pierrot, D., E. Lewis, and D. Wallace. 2006. MS Excel program developed for CO_2 system calculations. Carbon Dioxide Information Analysis Center, Oak Ridge National Laboratory, US Department of Energy. ORNL/CDIAC-IOS.

Powers, L. C., Hertkorn, N., McDonald, N., Schmitt-Kopplin, P., Del Vecchio, R., Blough, N. V., & Gonsior, M. (2019). Sargassum sp. Act as a Large Regional Source of Marine

Dissolved Organic Carbon and Polyphenols. *Global Biogeochemical Cycles*, *33*(11), 1423-1439.

Rangel, A.R. (2021). The Variability of Seawater Carbonate Chemistry in two Florida Urban Mangrove Ecosystems. Master's thesis. Nova Southeastern University. Retrieved from NSUWorks. (56)

Resiere, D., Valentino, R., Nevière, R., Banydeen, R., Gueye, P., Florentin, J., Cabié, A., Lebrun, T., Mégarbane, B., Guerrier, G., & Mehdaoui, H. (2018). Sargassum seaweed on Caribbean islands: an international public health concern. *The Lancet*, *392*(10165).

Rezanezhad, F., Couture, R. M., Kovac, R., O'Connell, D., & Van Cappellen, P. (2014). Water table fluctuations and soil biogeochemistry: An experimental approach using an automated soil column system. *Journal of Hydrology*, *509*, 245-256.

Rodil, I. F., Lastra, M., López, J., Mucha, A. P., Fernandes, J. P., Fernandes, S. V., & Olabarria, C. (2018). Sandy Beaches as Biogeochemical Hotspots: The Metabolic Role of Macroalgal Wrack on Low-productive Shores. Ecosystems, 22(1), 49-63.

Rodriguez-Martinez, R. E., Medina-Valmaseda, A. E., Blanchon, P., Monroy-Velazquez, L. V., Almazan-Becerril, A., Delgado-Pech, B., Vasquez-Yeomans, L., Francisco, V., & Garcia-Rivas, M. C. (2019). Faunal mortality associated with massive beaching and decomposition of pelagic Sargassum. *Mar Pollut Bull*, *146*, 201-205.

Rosentreter, J. A., Maher, D.T., Erler B.D., Murray, R.H., Eyre B.D. (2018). Methane emissions partially offset "blue carbon" burial in mangroves. *Science Advances*, *4*, 1-11.

Rosentreter, J. A., Maher, D. T., Erler, D. V., Murray, R., & Eyre, B. D. (2018). Seasonal and temporal CO_2 dynamics in three tropical mangrove creeks – A revision of global mangrove CO_2 emissions. Geochimica et Cosmochimica Acta, 222, 729-745.

Sansone, F.J., Martens C. S. (1982). Volatile fatty acid cycling in organic-rich marine sediments. *Geochimica et Cosmochimica 46*, 1575-1589.

Santos, I. R., Eyre, B. D., & Huettel, M. (2012). The driving forces of porewater and groundwater flow in permeable coastal sediments: A review. *Estuarine, Coastal and Shelf Science*, *98*, 1-15.

Sela-Adler, M., Ronen, Z., Herut, B., Antler, G., Vigderovich, H., Eckert, W., & Sivan, O. (2017). Co-existence of Methanogenesis and Sulfate Reduction with Common Substrates in Sulfate-Rich Estuarine Sediments. *Front Microbiol*, *8*, 766.

Shoener, A., Rowe G. T., (1970). Pelagic Sargassum and its presence among the deep-sea benthos. *Deep-Sea Research*, *17*, 923-925.

Siikamäki, J., Sanchirico, J. N., Jardine, S., McLaughlin, D., & Morris, D. (2013). Blue Carbon: Coastal Ecosystems, Their Carbon Storage, and Potential for Reducing Emissions. *Environment: Science and Policy for Sustainable Development*, *55*(6), 14-29.

Sippo, J. Z., Maher, D. T., Tait, D. R., Holloway, C., & Santos, I. R. (2016). Are mangroves drivers or buffers of coastal acidification? Insights from alkalinity and dissolved inorganic carbon export estimates across a latitudinal transect. *Global Biogeochemical Cycles*, *30*(5), 753-766.

Sippo, J. Z., Sanders, C. J., Santos, I. R., Jeffrey, L. C., Call, M., Harada, Y., Maguire, K., Brown, D., Conrad, S. R., & Maher, D. T. (2020). Coastal carbon cycle changes following mangrove loss. *Limnology and Oceanography*, *65*(11), 2642-2656.

Sissini, M. N., de Barros Barreto, M. B. B., Széchy, M. T. M., de Lucena, M. B., Oliveira, M. C., Gower, J., Liu, G., de Oliveira Bastos, E., Milstein, D., Gusmão, F., Martinelli-Filho, J. E., Alves-Lima, C., Colepicolo, P., Ameka, G., de Graft-Johnson, K., Gouvea, L., Torrano-Silva, B., Nauer, F., de Castro Nunes, J. M., . . . Horta, P. A. (2019). The floating Sargassum (Phaeophyceae) of the South Atlantic Ocean – likely scenarios. *Phycologia*, *56*(3), 321-328.

Sorrell, B. K., Downes, M.T., Stanger, C.L. (2002). Methanotrophic bacteria and their activity on submerged aquatic macrophytes. *Aquatic Botany, 72*, 107-119.

Thomas, H., Schiettecatte, L.S.,Suykens, K., Kon´e, Y.J.M., Shadwick, E.H., Prowe, A.E.F., Bozec, Y., de Baar, H.J.W., Borges, A.V. (2009). Enhanced ocean carbon storage from anaerobic alkalinity generation in coastal sediments. *Biogeosciences, 6*, 267-274.

Turner, J. P., & Rooker, J. R. (2006). Fatty acid composition of flora and fauna associated with Sargassum mats in the Gulf of Mexico. *Marine Biology*, *149*(5), 1025-1036.

van Tussenbroek, B. I., Hernandez Arana, H. A., Rodriguez-Martinez, R. E., Espinoza-Avalos, J., Canizales-Flores, H. M., Gonzalez-Godoy, C. E., Barba-Santos, M. G., Vega-Zepeda, A., & Collado-Vides, L. (2017). Severe impacts of brown tides caused by Sargassum spp. on near-shore Caribbean seagrass communities. *Mar Pollut Bull*, *122*(1-2), 272-281.

Wada, S., Aoki, M. N., Mikami, A., Komatsu, T., Tsuchiya, Y., Sato, T., Shinagawa, H., & Hama, T. (2008). Bioavailability of macroalgal dissolved organic matter in seawater. *Marine Ecology Progress Series, 370*, 33-44.

Wang, M., Hu, C., Barnes, B. B., Mitchum, G., Lapointe, B., Montoya, J.P. (2019). The great Atlantic Sargassum belt. *Science, 365*, 83-87.

Watanabe, K., Yoshida, G., Hori, M., Umezawa, Y., Moki, H., & Kuwae, T. (2020). Macroalgal metabolism and lateral carbon flows can create significant carbon sinks. *Biogeosciences*, *17*(9), 2425-2440.